

Circular Antenna Array Synthesis Using Fuzzy Genetic Algorithm

M. Bousahla¹, B. Kadri², F.T. Bendimerad¹

Abstract – This paper presents a rigorous synthesis of circular arrays of printed antennas using a hybrid fuzzy-genetic algorithm. Fuzzy logic based controllers are applied to fine-tune dynamically the crossover and mutation probability in the genetic algorithms, in an attempt to improve the algorithm performance. The FGA approach is compared with the Standard Genetic Algorithm(SGA). Included synthesis example clearly demonstrates that while the SGA approach gives satisfactory solutions for the problem, the FGA method usually performs significantly better. **Copyright © 2009 Praise Worthy Prize S.r.l. - All rights reserved.**

Keywords: Fuzzy genetic algorithms, population diversity measurements, circular antennas array, synthesis, fuzzy controller.

Nomenclature

p_m	mutation probability
p_c	crossover probability
D	whole diversity of population
D_g	gene diversity of population
D_{gw}	gene inner diversity
D_{gb}	gene outer diversity
D_i	individual diversity of population
D_{ib}	individual outer diversity
D_{iw}	individual inner diversity
\bar{P}_i	individuals average fitness
\bar{P}	average fitness of the population
\bar{f}	average fitness of the current population.
f_{\max}	fitness of the optimal individual
Number	frequency of the largest fitness value that is not changed
M	number of individuals in the population
l	length of string representing the individual
N	number of element in array.
φ_i	angular position of i^{th} Antenna
k_0	wave number.
R_i	distance between the i^{th} patch and the observation
(A_i, α_i)	complex excitation coefficients of the i^{th} patch
$E_{\text{tot}}(r, \theta, \phi)$	total radiated field of an array
$E(\theta, \phi)$	radiation pattern of one patch
d_i	i^{th} sample of the pattern in the beam region
d_{av}	average value in the beam region
Sll_{\max}	highest sidelobe level
fitness	fitness function of an individual

I. Introduction

The printed antennas array aroused an interest growing during these last years, in particular in the mobiles communications fields and the monolithic structures, where the radiating elements and the phase-converters are integrated in the same substrate. They also find applications in the space techniques to ensure a specific or partial terrestrial cover, like in the military and civil field.

This is mainly due to the unique feature of microstrip antennas; which are, namely, low in profile, compact in structure, light in weight, conformable to non planar surfaces, easy and inexpensive for mass production. The array association of several printed elements allows in addition an improvement of their performances, to accomplish a very particular functions, such as : scanning and beam steering, jamming rejection, adaptive detection, autoadaptativity, carrying out of various radiation patterns, the directivity pattern and polarization control, ...etc.

The circular array, in which the radiating elements are placed on circular rings, is an array of very great practical interest. These applications are multiple: radars, sonar, terrestrial and space navigation and much of other systems [1-2].

The application of genetic algorithms GAs as optimization tools for the design of antennas has been an active field of search in the past decade [3-4]. They have roved to be a useful and powerful alternative to traditional optimization techniques [5-7] when handling with multidimensional, multimodal optimization problems, and their success is related to versatility, robustness and ability to optimize non differentiable cost function [3,8-9].

The performances of the genetic algorithm is correlated to directly with its careful selection of parameters. It is possible to destroy an high fitness

individual when a large crossover probability is set. The performance of the algorithm would fluctuate significantly. For a low crossover probability, sometimes it is hard to obtain better individuals and does not guarantee faster convergence. High mutation introduces too much diversity and takes longer time to get the optimal solution. Low mutation tends to miss some near-optimal points.

Adaptive genetic algorithms, which dynamically adapt selected control parameters or genetic operators during the evolution, have been built to avoid the premature convergence problem and improve GA behaviour. One of the adaptive approaches is the parameter setting techniques based on the use of fuzzy logic controllers (FLCs), the fuzzy genetic algorithm (FGA) [8-11].

In this paper we develop the synthesis of the complex radiation pattern of a circular antenna array with probe feed by optimizing amplitude excitation coefficients, the desired radiation pattern is specified by a narrow beam pattern with a beam width of 8 degrees and a maximum side lobe levels of -30dB pointed at 0°. The simulation results obtained while applying FGAs are compared, in the same conditions, with those obtained by the standard genetic algorithms SGAs.

In section 2 we present the design method of the proposed optimization technique, the design of a fuzzy controller is discussed to adjust crossover and mutation probabilities according to the population diversity measurements and the best fitness individual.

The synthesis problem of a circular antenna array with rectangular cells using FGAs by optimization of the complex excitation coefficients is presented in section 3.

In section 4: numerical results for a circular array using both the SGAs and FGAs are presented to compare the performances obtained while introducing fuzzy techniques in GAs. Finally, some conclusions are drawn in section 5.

II. Fuzzy Genetic Algorithms

Genetic algorithm was proposed by Holland in the 1970s [3], which is an optimization algorithm simulating natural evolution. Although GA becomes very famous with its global searching, parallel computing, better robustness, and not needing differential information during evolution.

GAs include three primary genetic operators: selection, crossover and mutation. Selection embodies the principal of 'Survival of the fitness'. The attention of crossover is to recombine genetic material of parents to form their offspring and to reach the new regions in search space [10-11]. The role of mutation in GAs has been that of restoring lost or unexpected genetic material into population to prevent premature convergence of the GA to sub-optimal solutions.

However, GA has also some demerits, such as poor local searching, premature converging as well as slow convergence speed.

The GAs behavior is determined by the exploitation and exploration relationship kept throughout the GA run. This balance between the utilization of the whole solution space and the detailed searching of some parts can be adapted to change of GA operators setting (selection, crossover and mutation). So, different genetic operators or control parameters values maybe necessary during the course of a run for inducing an optimal exploration/exploitation balance. For these reasons, adaptive genetic algorithms (AGAs) have been built that dynamically adjust selected control parameters or genetic operators during the course of evolving a solution [10-11].

One way for designing AGAs involves the application of fuzzy logic controller (FLCs) [10,11] for adjusting GA control parameters.

The main idea of adaptive GAs based on fuzzy controllers FLCs is to use a FLC whose inputs are any combination of GA performance measures or current control parameters and whose outputs are GA control parameters. Current performance measures of the GA are sent to the FLC, which computes the new control parameters values that will be used by the GA as demonstrated by the flow chart shown in figure 1.

FLC's inputs should be robust measures that describe GA behavior and the effects of genetic setting parameters and genetic operators, some possible inputs were cited in [10,11]: diversity measures, maximum, average, minimum fitness.

FLC's outputs indicate the values of control parameters or changes in these parameters, the following outputs were reported in [11]: mutation probability, crossover probability, population size ... etc.

We have chosen for FLC's outputs p_c and p_m to realize the twin goals of maintaining diversity in population and sustaining the convergence capacity of the GA [10,11].

II.1. Fuzzy logic controller design

Most AGAs based on FLCs presented in literature [9-11] involve population level adaptation, by adjusting control parameters that apply for entire population. The premature convergence of GAs depends on PD descending quickly which can be prevented through controlling PD to maintain proper value.

The FLC design takes into account the PDM and a performance measure of GAs, in this paper the FLC has three inputs (D_{gw} , \bar{f}/f_{max} and Number) and two outputs (p_c and p_m) as indicated in figure 2.

Next we derive how we can compute the PDM for a given population.

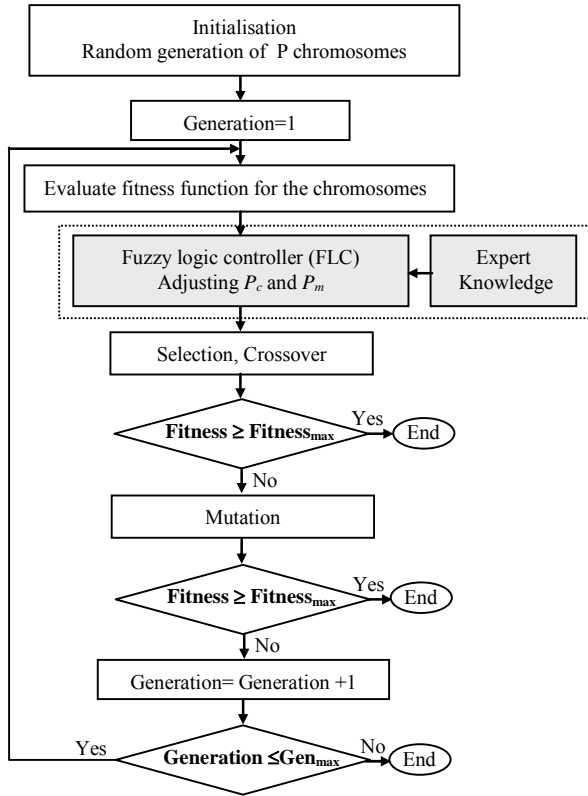


Fig. 1. Flowchart of the fuzzy genetic algorithms FGAs.

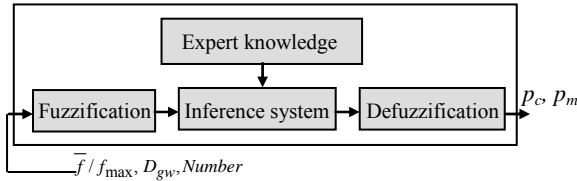


Fig. 2. Structure of the fuzzy logic controller FLC.

II.2. Population diversity measurements

Lets take a population P using a binary encode to be presented by a $M \times l$ matrix, every row of matrix presents an individual string, and the column presents the value of every individual string at the special gene bit, so, p_i^j represents the j^{th} bit gene value of the i th individual string.

Expressions derived here for computing PDM are inspired from the work of Kejung Wang [11], where it was demonstrated that the whole diversity of population D can be decomposed into two different meaning and effect diversity as given by equation 1:

$$D = \frac{1}{M.l} \cdot \sum_{i=1}^M \sum_{j=1}^l (p_i^j - \bar{P})^2 = D_i = D_g \quad (1)$$

where \bar{P} is given by :

$$\bar{P} = \frac{1}{M.l} \cdot \sum_{i=1}^M \sum_{j=1}^l p_i^j \quad (2)$$

By means of \bar{P}_i the individual diversity of population may be decomposed into two terms as given by (3) :

$$D_i = D_{iw} + D_{ib} \quad (3)$$

D_{iw} indicates the discrepancy between the genes in every individual and the individual average, and reflects the diversity of one individual inner composition, D_{iw} is given by (4):

$$D_{iw} = \bar{\delta}_2 = \frac{1}{M.l} \sum_{i=1}^M \sum_{j=1}^l (p_i^j - \bar{P}_i)^2 \quad (4)$$

D_{ib} indicates the discrepancy between the average of all individuals and the population average, it is the diversity among different individuals, and reflects the discrepant degree among different individuals, D_{ib} is given by (5):

$$D_{ib} = \delta \bar{P} = \frac{1}{M} \sum_{i=1}^M (\bar{P}_i - \bar{P})^2 \quad (5)$$

And by means of the gene average \bar{g}^j (7) the gene diversity of population may be decomposed into two terms as given by (6) :

$$D_g = D_{gw} + D_{gb} \quad (6)$$

$$\bar{g}^j = \frac{1}{M} \cdot \sum_{i=1}^M p_i^j \quad (7)$$

The gene inner diversity which indicates the discrepancy average among the individual value at the special gene bit in population and reflects the convergent degree at this gene bit. D_{gw} is computed by (8):

$$D_{gw} = \bar{\delta}_1 = \frac{1}{M.l} \sum_{i=1}^M \sum_{j=1}^l (p_i^j - \bar{g}^j)^2 \quad (8)$$

D_{gb} indicates the discrepancy between the average value of all gene bits and the population average, that is the discrepancy among gene average, D_{gb} is calculated by (9):

$$D_{gb} = \delta \cdot \bar{g} = \frac{1}{l} \sum_{i=1}^M \left(\bar{g}^j - \bar{P} \right)^2 \quad (9)$$

In the research of GAs convergence, we pay close attention to the former the gene inner diversity. It represents the genetic drift degree and is the important criterion of GAs evolution ability.

D_{gw} represents the genetic drift degree and evolution ability of current population. \bar{f} / f_{max} is used to judge

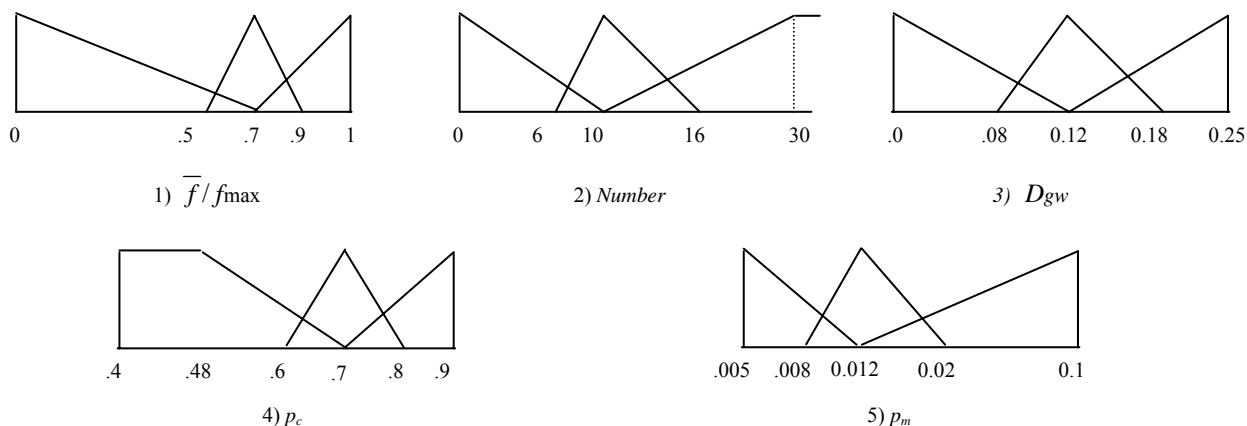


Fig. 3. The membership functions of inputs and output.

whether the current PD is useful [11]], if it's near to 1, convergence has been reached, whereas if it's near to 0, the population shows a high level of diversity[10-12]. Number is used to record the frequency of the largest fitness value that is not changed.

The input variables D_{gw} , \bar{f}/f_{max} and Number to be included respectively in the ranges : [0 , 0.25], [0 , 1] and [0 , 30]. For the FLC's outputs practical values of p_c and p_m are chosen and are included respectively in the ranges: [0.4, 0.9] and [0.005, 0.1].

II.3. The membership functions of inputs and outputs

Each input and output should have an associated set of linguistic labels. The meaning of these labels is specified through membership functions of fuzzy sets.

The linguistic value sets of inputs and outputs are all: { *LOW*, *MEDIUM*, *HIGH* }.

According to the changing scope of input variables and output variables in FLC, and their linguistic value sets, we have adopted the same membership functions of inputs and outputs as given by [11]. Triangular membership functions and non-homogenous demarcation are adopted as it is illustrated in figure 3.

II.4. Fuzzy control rules

After selecting the inputs, the outputs and defining the database, the fuzzy rules describing the relations between them are derived and are given in the table 1 [11].

Referring, for example, to the first line in the table 1, if we consider \bar{f}/f_{max} low which means that we are far from the optimum (the best) and D_{gw} is low which signifies that all individuals surround (or gather around) one point. In this case the actual population is bad and we must favourite more and more crossover and mutation by choosing high values of p_c and p_m .

The fuzzy logical system uses a triangular membership functions, the min intersection operator and correlation-product inference procedure. Fuzzification of inputs was performed using the single value fuzzy production. Defuzzification of the outputs was performed using the fuzzy center average method.

Once the GAs optimized by a fuzzy controller based on the use of the population diversity measurements is defined, we use this algorithm in the synthesis of linear microstrip antenna array.

TABLE I
FUZZY CONTROL RULES (p_w/p_c)

\bar{f}/f_{max}	Number	D_{gw}	p_m	p_c
LOW	-	LOW	HIGH	HIGH
LOW	-	MEDIUM	HIGH	MEDIUM
LOW	-	HIGH	MEDIUM	HIGH
MEDIUM	-	LOW	HIGH	MEDIUM
MEDIUM	-	HIGH	LOW	MEDIUM
HIGH	LOW	-	LOW	HIGH
HIGH	MEDIUM	LOW / MEDIUM	LOW	MEDIUM
HIGH	HIGH	LOW	LOW	LOW
MEDIUM / LOW	LOW	-	LOW	HIGH
MEDIUM	MEDIUM / HIGH	-	LOW	MEDIUM
LOW	LOW	-	MEDIUM	HIGH
LOW	MEDIUM / LOW	-	HIGH	MEDIUM
-	LOW	MEDIUM / HIGH	LOW	HIGH
-	HIGH	MEDIUM / HIGH	LOW	MEDIUM

III. Synthesis of Circular Antenna Array

Synthesis of a circular antenna array by the determination of amplitude excitation coefficients to best meet a specified far-field radiation pattern has been already presented [13-14].

We develop in this paper the synthesis of a circular antenna array with probe feed using the FGAs discussed in the previous section.

Let us consider a circular array consisting of N radiating elements distributed regularly on a circle of radius R_c , in the xOy plane as show in figure 4.

Let us consider an array of N isotropic elements placed on a circular ring of radius R_c , lying on the $x-y$ plane of an orthogonal Cartesian system $O(x,y,z)$. The n -th element of the array is located at ϕ_i with the x axis, where $\phi_i = 2.\pi.iN^{-1}$, $i=1,2,\dots,N$.

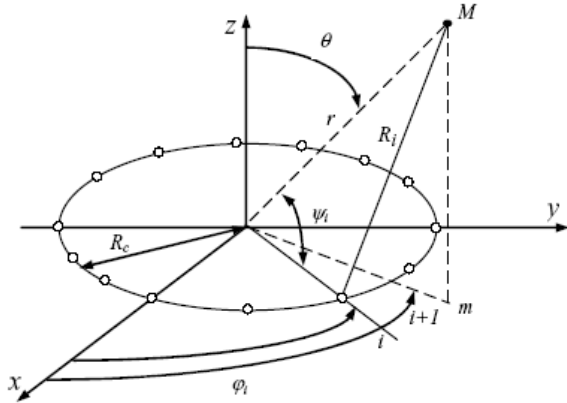


Fig. 4. Circular array of N elements

We consider the total radiated field $E_{tot}(r, \theta, \phi)$ of the array in the plane of array as the result of a sum of the contribution of each element in the observed direction. We can then write [7]:

$$E_{tot}(r, \theta, \phi) = \sum_{i=1}^N w_i \cdot \frac{e^{-jk_0.R_i}}{R_i} \cdot E(\theta, \phi) \quad (10)$$

$$= \frac{e^{-jk_0.R_i}}{R_i} \sum_{i=1}^N w_i \cdot e^{-jk_0.R_c \cdot \sin \theta \cos(\phi - \phi_i)} \cdot E(\theta, \phi)$$

where:

$$R_i \cong r - R_c \cos \psi_i \cong r - R_c \sin \theta \cos(\phi - \phi_i) \quad (11)$$

$$w_i = A_i \cdot e^{j\alpha_i} \quad (12)$$

The radiation field of an elementary source $E(\theta, \phi)$ is computed using the two-slot model by modeling the antenna as a combination of two parallel slots of length W , width h , and spaced a distance L apart as described in [15]. The radiation from the patch is linearly polarized with the electric field directed along the patch length.

We can obtain finally:

$$E_{tot}(r, \theta, \phi) = \frac{e^{-jk_0.r}}{r} \sum_{i=1}^N A_i \cdot e^{-j(k_0.R_c \cdot \sin \theta \cos(\phi - \phi_i) + \alpha_i)} \cdot E(\theta, \phi) \quad (13)$$

According to the desired performances, we can consider an array comprising several rings. Among the various manners of setting out again the elements, one chose a distribution as show in Figure 5.

The circle which presents the smallest ray must check the weakest spacing between the sources ($d_1 = 0.6\lambda$). The spacing between the circles is of $d_2 = 0.6\lambda$ (λ being the wavelength number related to the operating frequency).

The total radiated field in this case is:

$$E_{tot}(r, \theta, \phi) = E(\theta, \phi) \sum_{i=1}^M \sum_{j=1}^N w_{ij} \cdot e^{-jk_0.R_{ci} \cdot \sin \theta \cos(\phi - \phi_{ij})} \quad (14)$$

We use the FGAs to find the amplitude excitation vector $A = [A_1, A_2, \dots, A_N]$ so the radiation pattern produced satisfy the desired radiation pattern specified by the pattern model as illustrated in the figure 6, we suppose that all patches have the same excitation phase(null phase). This pattern has a narrow beam with -30 dB sidelobes. The pattern is normalized to the peak value at 0 degrees and must have a 3dB beamwidth of at least 8 degrees. The -30 dB sidelobe level must be met beginning at ± 10 degrees and extending to ± 90 degrees. The sidelobes in this case are defined relative to the peak of beam at 0 degrees. The specifications are illustrated in figure 6.

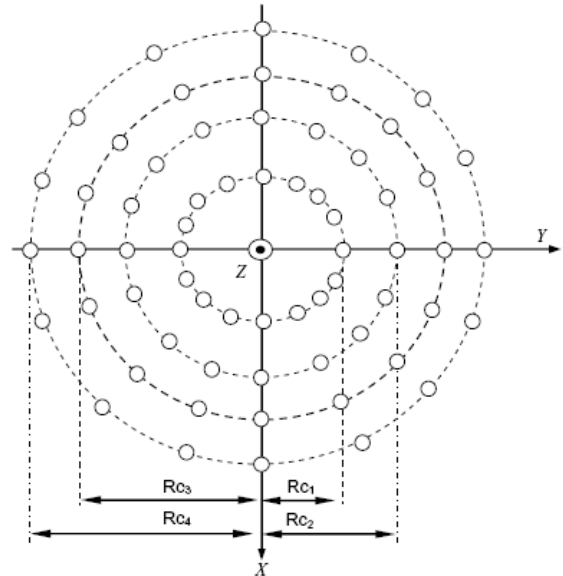


Fig. 5. Circular array with several rings.

We have choose a suitable fitness function that can guide the SGAs and FGAs optimization toward a solution that meets the desired radiation pattern as mentioned in [16]. Equations 15-17 describe the appropriate fitness function.

$$d_{av} = \frac{1}{2S+1} \sum_{i=-S}^S d_i \quad (15)$$

$$Sll_{\max} = \min_{\forall i \in \text{Sidelobes}} (d_{av} - d_i) \quad (16)$$

$$fitness = d_{av} + w_1 Sll_{\max} \quad (17)$$

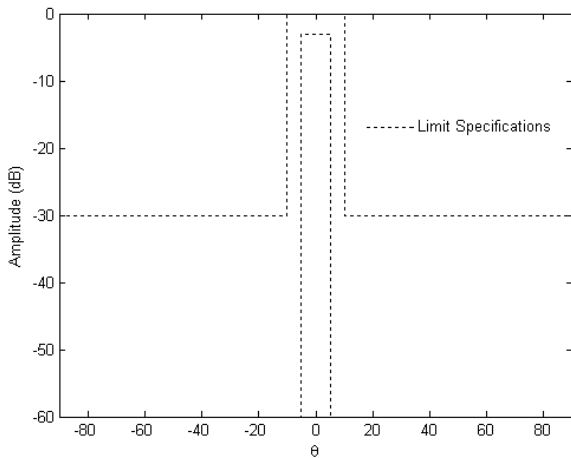


Fig. 6. Plot of the desired pattern specifications.

Where it is assumed that a number of samples of the pattern, d_i in dB, are taken in the beam region and the sidelobe region and that the number of samples in the beam region is equal to $2S+1$. An arbitrary weight w_1 is used, the goal of function (17) is to maximize the difference between d_{av} and Sll_{\max} .

First we have to find a relationship between the GAs and the array. In the case of a coded GA, each element of the array is represented by a string of bits which gives the amplitude excitation of the element; hence each element is characterized by its amplitude excitation. This relationship is shown in table 2.

TABLE II.
RELATIONSHIPS BETWEEN ELEMENTS OF GAS AND ARRAYS.

Genetic parameters	Antennas array
Gene	Bits chain(string): Amplitude
Chromosome	One element of array
Individual	One array
Population	Several arrays

IV. Numerical results

We have considered a circular array of radius $R_c = 2\lambda$, consisting of $N=96$ elements organized on six concentric rings, using the above techniques we have synthesized the pattern reproduced on figure 6. In our simulation, we have used a population size of 40 for GAs. Roulette strategy for "selection", one-point crossover and mutation to flip bits.

For the SGAs, we have used value of $p_c=0.75$ and $p_m=0.03$.

For the FGAs, p_c and p_m are determined according to FLC given in section 2.1.

We have adopted a desired radiation pattern specified by a narrow beam pointed at 0 degrees as illustrated in figure 6. Figures 7 to 12 show an example of synthesis of a probe-fed circular array constituted by 96 rectangular microstrip antennas with 0.906cm width and 1.186cm long working at the frequency of 10GHz, the array is printed on a substrate with 1.1588mm height and a dielectric constant equal to 2.2.

In figure 7 we present the result of circular array optimization by magnitude excitation coefficients using both SGAs and FGAs. It is clearly seen that the radiation pattern obtained by FGAs meet better the desired pattern than obtained by SGAs. The optimized amplitude excitation coefficients by both optimizer algorithms are reproduced on figure 9 and 10.

The best fitness function obtained by FGAs is better than the obtained by a SGAs, this is shown in figure 8.

For each generation the probabilities p_c and p_m are adjusted according to the response of the fuzzy controller, and shown in figures 11 and 12.

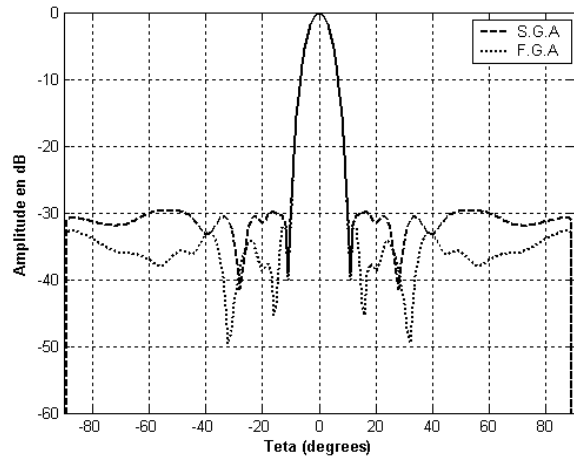


Fig. 7. Result of a circular array synthesis with 96 rectangular microstrip antennas fed by coax applying both SGAs and FGAs.

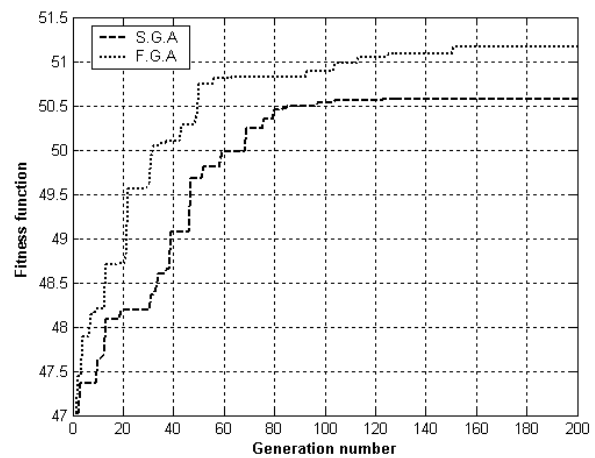


Fig. 8. Comparison between fitness function obtained by the two algorithms SGAs and FGAs.

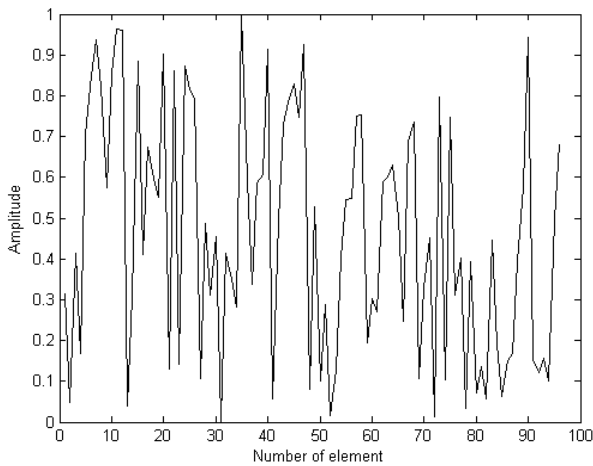


Fig. 9. Optimized amplitude excitation coefficients by SGAs.

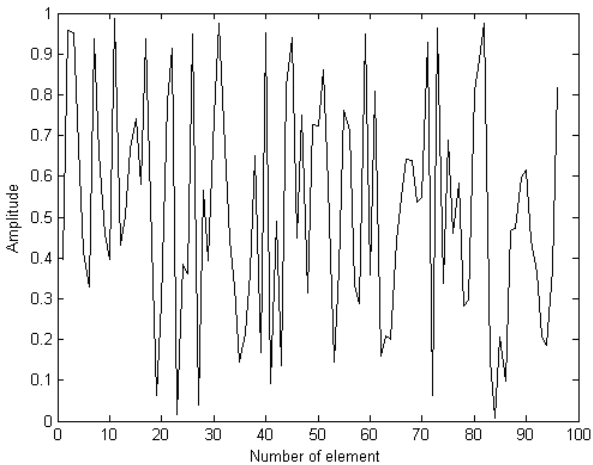


Fig. 10. Optimized amplitude excitation coefficients by FGAs.

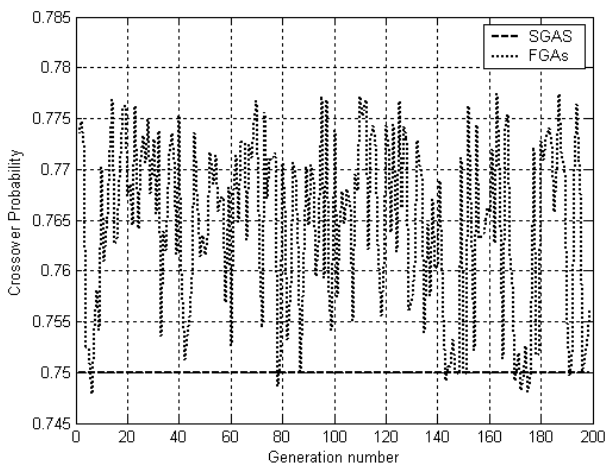


Fig. 11. Adjusting p_c during GAs run.

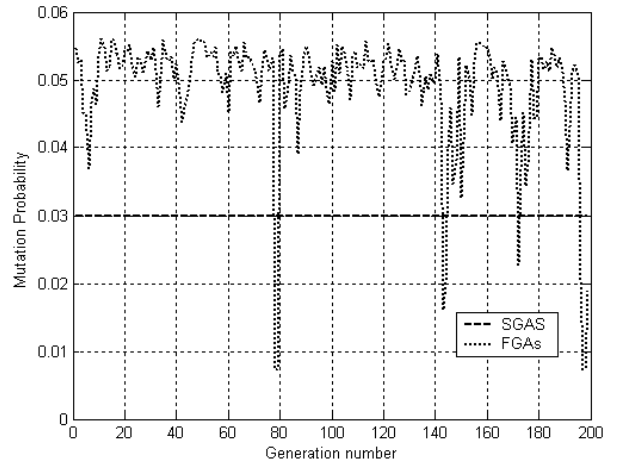


Fig. 12. Adjusting p_m during GAs run.

V. Conclusion

We have developed in this paper the synthesis of a probe-fed circular array using adaptive genetic algorithms whose control parameters are dynamically adjusted by the use of fuzzy controller.

The standard genetic algorithms SGAs are subject to premature convergence problem, which is due to: control parameter not well chosen initially for a given task, parameters always being fixed even though the environment in which GA operate may be variable.

The FGAs has been built for inducing exploitation/exploration relationships that avoid premature convergence problem by optimizing the parameters controlling the GAs like crossover and mutation probabilities depending on the measure of population diversity PD.

The SGA converges quickly with a larger probability to get trapped in local optima, while the FGA spends more time to explore ore feasible solutions with a larger probability to find global optimal solutions.

As seen in the simulation example of the circular antenna array synthesis, the performances of FGAs are much better than the SGAs in terms of: approaching better the specified desired radiation pattern and the high speed approaching of the global optimal.

References

- [1] PRASAD, s., and CHARAN, R., On the constrained synthesis of array patterns with applications to circular and arc arrays, *IEEE Trans.*, 1984, AP-32, (7), pp. 725-730
- [2] KARAVASSILIS, N., DAVIES, D.E.N., and GUY, c.G.: Experimental HF circular array with direction finding and null steering capabilities, *IEE Proc. H*, 1986, 133, (2), pp. 147-154
- [3] R. L. Haupt, An Introduction to Genetic Algorithms for Electromagnetic, *IEEE Antenna and propagation Magazine*, Vol. 37, pp. 7-15, 1995.

- [4] D. Marcano, F. Duran, Synthesis of Antenna Arrays Using Genetic Algorithms, *IEEE Antenna and propagation Magazine*, Vol. 42, NO. 3, June 2000.
- [5] D.K. Cheng, "Optimization techniques for antenna arrays", Proc IEEE 59 (1971), 1664-1674.
- [6] B. Kadri, F.T. Bendimerad, E. Cambiaggio, Synthèse Rigoureuse D'antennes Microrubans en Réseau non Périodique par Modélisation des Circuits d'Alimentations, 10^{ème} Journées Internationales de Nice sur les Antennes, *JINA'98, International Symposium*, pp. 358-361, Nice 17-19 Novembre 1998.
- [7] B. Kadri, F.T. Bendimerad, E. Cambiaggio, Modelisation of the Feed Network Application to Synthesis Unequally Spaced Microstrip Antennas Arrays, *International Conference on Electromagnetics in Advanced Applications (ICEAA 99)*, pp. 371-374, Torino, 13-17 September 1999.
- [8] D. Marcano, F. Duran, Synthesis of antenna arrays using genetic algorithms, *IEEE Antennas Propagat Mag* 42 (2000).
- [9] M. Donelli, S. Coarsi F. De Natale, M. Pastorino, A. Massa, Linear Antenna Synthesis With Hybrid Genetic Algorithm, *Progress in Electromagnetics Reaseach, PIER 49*, 1-22, 2004.
- [10] F. Herrera, M. Lozano, Adaptive Genetic Operators Based On Coevolution With Fuzzy Behaviors, *IEEE Transaction on Evolutionary Computation*, Vol. 5, NO. 2, April 2001.
- [11] K. Wang, A New Fuzzy Genetic Algorithm Based on Population Diversity, *International Symposium on Computational Intelligence in Robotics and Automation*, pp. 108-112, July 29 August 1, 2001, Alberta, Canada.
- [12] F. Herrera et M. Lozano, Adaptive genetic algorithms based on fuzzy techniques, *Information Proceedings and Management of Uncertainly in Knowledge-Based Systems*, pages 775-980, 1996.
- [13] VESCOVO, R.: Constrained and unconstrained synthesis of array factor for circular arrays, *IEEE Trans.*, 1995, AP-43, (12), pp. 1405-1410
- [14] VESCOVO, R., and CARLI, E., Null control of pattern for circular antenna arrays, *Proc. 25th European Microwave Conf.*, 1995, 1, pp. 36 9-371
- [15] R. Garg, P. Bhartia, I. Bahl, A. Ittipiboon, *Microstrip Antenna design Handbook* (Artech House INC, ISBN 0-89006-513-6, 2001).
- [16] R. L. Haupt, J. M. Johnson, Dynamic Phase-Only Array Beam Control Using a Genetic Algorithm, *evolvable Hardware (EH'99)*, 217-224, July 19-21, Pasadena, CA, USA, IEEE Computer Society 1999.

heuristic algorithms.



Fethi Tarik Bendimerad was born in Sidi BelAbbès, Algeria, in 1959, he received his Phd degree from the Sophia-Antipolis University in Nice (France), in 1989. He is currently a full professor at the Faculty of engineering at the Abou BekrBelkaid University in Tlemcen, (Algeria) and the Director of the Telecommunications Laboratory. His field of interest is antenna treatment and smart antenna.

Authors' information

¹Abou-Bakr Belkaid University, Telecommunications Laboratory, Algeria

²Bechar University, Sciences and technologies Faculty, 08000, Bechar, Algeria



Miloud Bousahla was born in Sidi BelAbbès, Algeria, in 1969. He received the Magistère diplomas in 1999 from Abou BekrBelkaid University in Tlemcen (Algeria). He is currently a Junior Lecturer in the Abou BekrBelkaid University. Also he is a Junior Researcher within the Telecommunications Laboratory. He works

on design, analysis and synthesis of antenna and conformal antenna and their applications in communication and radar systems



Boufeldja Kadri was born in Bechar, Algeria, in 1972. He received the Majister degree in 1998, from the Abou Bekrbelkaid University in Tlemcen (Algeria). Since 1999, he joined the Electronic Institute in Bechar University (Algeria), where he is now an associate professor. His research interests include modeling and optimization of antenna array with

Synthesis of Circular Arrays with Simulated Annealing Optimization Algorithm

M. Bousahla, M. Abri, F. T. Bendimerad and N. Boukli-hacene

*Laboratoire de Télécommunications, Département d'Electronique
Faculté des Sciences de l'Ingénieur, Université Abou-Bekr Belkaïd -Tlemcen
BP 230, Pôle Chetouane, 13000 Tlemcen- Algeria*

Abstract

This paper presents an analysis and a synthesis of circular arrays of printed antennas. The simulated annealing technique which is a probabilistic methodology to solve combinatorial optimization problems, has been applied to optimize the amplitude of weights coefficients of the elements of the circular array in order to improve the antenna performances and to obtain a beam pattern that meet given requirements. It is seen that the optimization method is effective in designing such arrays. The power of the simulated annealing method lies in its ability to avoid the local minima and to converge to the global minimum of the cost function, thanks to the exploitation of simulated annealing potentialities and high flexibility.

Key words: Printed antennas, circular arrays, analysis, synthesis, simulated annealing.

Introduction

The printed antennas array aroused an interest growing during these last years, in particular in the mobiles communications fields and the monolithic structures, where the radiating elements and the phase-converters are integrated in the same substrate. They also find applications in the space techniques to ensure a specific or partial terrestrial cover, like in the military and civil field. This is mainly due to the unique feature of microstrip antennas; which are, namely, low in profile, compact in structure, light in weight, conformable to non planar surfaces, easy and inexpensive for mass production.

The array association of several printed elements allows in addition an improvement of their performances, to accomplish a very particular functions, such

as: scanning and beam steering, jamming rejection, adaptive detection, autoadaptativity, carrying out of various radiation patterns, the directivity pattern and polarization control, ...etc.

The circular array, in which the radiating elements are placed on circular rings, is an array of very great practical interest. These applications are multiple: radars, sonar, terrestrial and space navigation and much of other systems [1]-[2].

In the antennas arrays domain, the synthesis problem consists in estimating the variations of the feeding weights of the radiating elements which permits to provide a radiation pattern as close as possible to a desired pattern specified by a shape pattern. The goal of this optimization is to seek for the optimal amplitude according to a precise specification. In this domain, many deterministic synthesis tools were developed. Taking into account the diversity of the goals sake by the users, one will not find a general synthesis method applicable to all cases, but rather a significant number of specific methods to each type of problem. Recently, global stochastic optimization techniques appeared, able to obtain global optima, without remaining trapped on local optima as is in the case for the deterministic methods. To achieve this goal we developed a synthesis method of these arrays by employing an optimization method based on the simulated annealing technique (SA). Simulated annealing is presented as method of finding optimal or near-optimal solutions to problems for which rigorous optimization method do not exist. The literature has reported the application of SA for general electromagnetic problems and, particularly, for the arrays synthesis [3]-[6].

This paper is organized as follows, in section II, the total radiated field of the circular array is determined and plotted in 2D and 3D. Section III presents the synthesis problem. Section IV describes the proposed method of synthesis and its basic concepts are summarized. The obtained results are reported in section V. Finally, conclusions are drawn in section VI.

Analysis

A circular array consists of N radiating elements distributed regularly on a circle of radius R_c , in the xOy plane as show in Fig. 1.

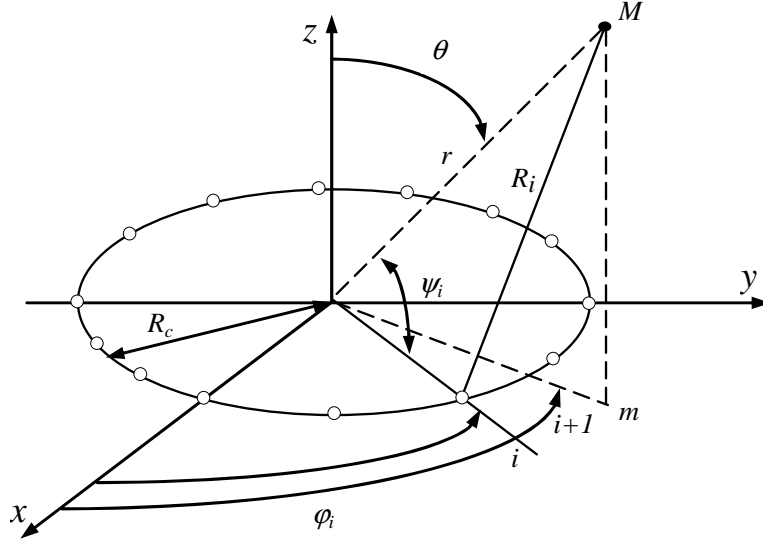


Figure 1: Circular array of N elements.

We consider the total radiated field $E_{tot}(r, \theta, \phi)$ as the result of a sum of the contribution of each element in the observed direction. We can then write [7]:

$$E_{tot}(r, \theta, \phi) = \sum_{i=1}^N w_i \frac{e^{-jk_0 R_i}}{R_i} E(\theta, \phi) = \frac{e^{-jk_0 R_i}}{R_i} \sum_{i=1}^N w_i e^{-jk_0 R_c \sin \theta \cos(\phi - \phi_i)} E(\theta, \phi) \quad (1)$$

With:

$$\phi_i = 2\pi \left(\frac{i}{N}\right) \text{ and } w_i = A_i e^{j\alpha_i}$$

We can obtain finally:

$$E_{tot}(r, \theta, \phi) = \frac{e^{-jk_0 r}}{r} \sum_{i=1}^N A_i e^{-j(k_0 R_c \sin \theta \cos(\phi - \phi_i) + \alpha_i)} E(\theta, \phi) \quad (2)$$

To fulfil the electronic sweeping function with such a device and to thus place the main lobe radiation in a direction (θ_0, ϕ_0) , it is necessary that the term α_i check the equation (3).

$$\alpha_i = -k_0 R_c \sin \theta_0 \cos(\phi_0 - \phi_i) \quad (3)$$

The total radiated field can be written:

$$\begin{aligned} E_{tot}(r, \theta, \phi) &= \frac{e^{-jk_0 r}}{r} \sum_{i=1}^N A_i e^{jk_0 R_c (\sin \theta \cos(\phi - \phi_i) - \sin \theta_0 \cos(\phi_0 - \phi_i))} E(\theta, \phi) \\ &= \frac{e^{-jk_0 r}}{r} \times \sum_{i=1}^N A_i e^{jk_0 d_0 \cos(\phi_i - \zeta)} E(\theta, \phi) \end{aligned} \quad (4)$$

With:

$$\zeta = \operatorname{arctg} \left\{ \frac{\sin \theta \sin \phi - \sin \theta_0 \sin \phi_0}{\sin \theta \cos \phi - \sin \theta_0 \cos \phi_0} \right\} \quad (5)$$

and

$$d_0 = R_c \left[(\sin \theta \cos \phi - \sin \theta_0 \cos \phi_0)^2 + (\sin \theta \sin \phi - \sin \theta_0 \sin \phi_0)^2 \right]^{\frac{1}{2}} \quad (6)$$

According to the desired performances, we can consider an array comprising several crowns. Among the various manners of setting out again the elements, one chose a distribution as show in Fig. 2.

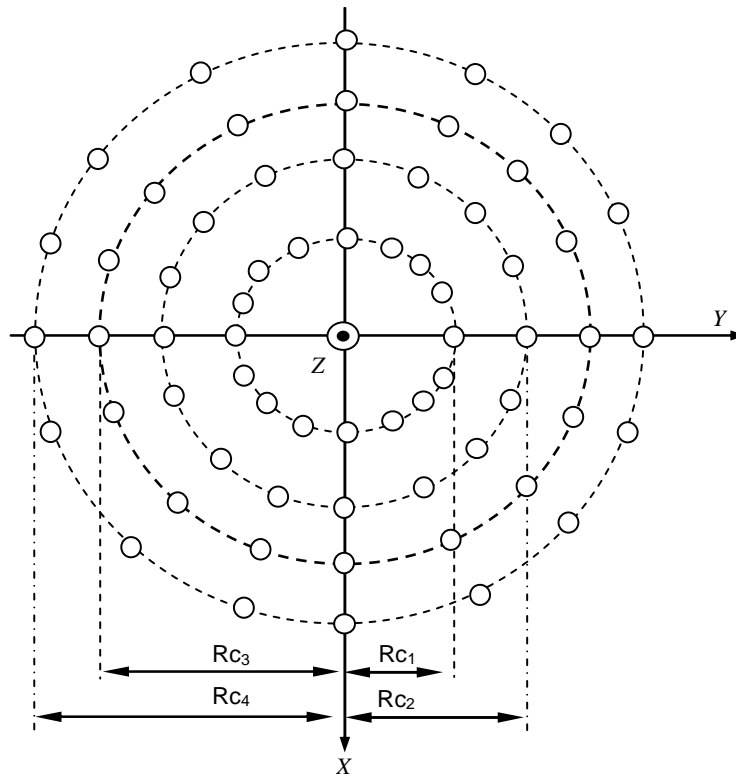


Figure 2: Circular array with several crowns.

The circle which presents the smallest ray must check the weakest spacing between the sources ($d_1 = 0.6\lambda$). The spacing between the circles is of $d_2 = 0.6\lambda$ (λ being the wavelength number related to the operating frequency).

The total radiated field in this case is:

$$E_{tot}(r, \theta, \phi) = E(\theta, \phi) \sum_{i=1}^M \sum_{j=1}^N w_{ij} e^{-jk_0 R_{c_i} \sin \theta \cos(\phi - \phi_{ij})} \quad (7)$$

Synthesis problem

The synthesis problem in which one is interested consists in minimizing the levels of the harmful side lobes to the useful radiation [7]-[10].

$$W_i = A_i e^{-j\varphi_i} \quad (8)$$

Where:

W_i are complex weights to each element.

A_i is the amplitude of the excitation and φ_i is the phase of the excitation.

The synthesis consists of minimizing a criterion of variation δ between the synthesized pattern $F_s(\theta, \varphi)$ and the desired pattern $F_d(\theta)$ defined by a shape pattern imposed in advance by the user. The optimization problem then consists in minimizing the quadratic error.

$$\delta(\theta, \varphi) = \sum_{\theta} |F_s(\theta, \varphi) - F_d(\theta)|^2 \quad (9)$$

Where :

F_d is the desired function and F_s is the synthesized function.

The SA described in next section, has been found to be very effective for the optimization of the array, thanks to its robustness and inherent ability to accommodate a variety of constraints.

Basic concepts of simulated annealing

SA is a probabilistic method based on concepts deriving from statistical mechanics by the means of the famous method of annealing used by the metallurgists. This method uses the Metropolis algorithm [11]. This algorithm is precisely used to randomly draw a continuation from microscopic configurations by respecting the proportions of Boltzmann relating to balance at a given temperature. As for the algorithm of iterative improvement, the algorithm of Metropolis makes it possible to explore by a random walk a graph whose tops are the microscopic configurations of the system.

In the case of the iterative improvement, displacement in the graph is always carried out towards the configurations of decreasing cost, while the algorithm of Metropolis allows sometimes transitions towards configurations from higher cost. In optimization, an iterative research which accepts only the new points corresponding to a lower value of the function is equivalent to a physical system which reaches temperature equal to zero quickly, which brings us at local minima. On the other hand simulated annealing seeks to converge towards the global minimum thanks to the control of the parameter temperature.

The algorithm of Metropolis calculates the new function $E_{new} = f(x_1)$, with x_1 the new point generated starting from a function $g(\Delta x)$ where Δx is the difference between the new point and the current point.

The majority of the optimization methods using simulated annealing choose their new point with variable distances from their starting point or running. If the solution obtained is better than the preceding one, then this solution is accepted. If the

preceding solution remains better, a law of probability of acceptance intervenes in order to decide to keep or reject this value.

Probability of acceptance determined by a function H , depends on the temperature T and difference between the two values of the function. As an example, while referring to the Boltzmann law, definite as follows [12]:

$$H = \frac{1}{1 + \exp(\Delta E/T)} \approx \exp(-\Delta E/T) \quad (10)$$

Where $E = f(x)$ represent the system energy, and $\Delta E = E_{new} - E$ represent the difference in energy between the new point and the preceding point.

In order to accept or to reject a point for which E_{new} is not better than E , one carries out the lots of a random variable P on $[0, 1]$. If the variable obtained is lower than H the point is then accepted. In the contrary case, the new point is refused.

When a new point is accepted, even if the corresponding value of the function is worse than with the preceding point, it becomes then the new point running or solution. At the beginning, the temperature T must be large and a new point must be roughly accepted once on two. With the progression of the algorithm in time, the temperature T is reduced, implying a fall of the acceptance probability of the points. In fact, the value called ‘‘temperature’’ T is only one parameter making it possible to control the amplitude of the movements and makes it possible to avoid the minima.

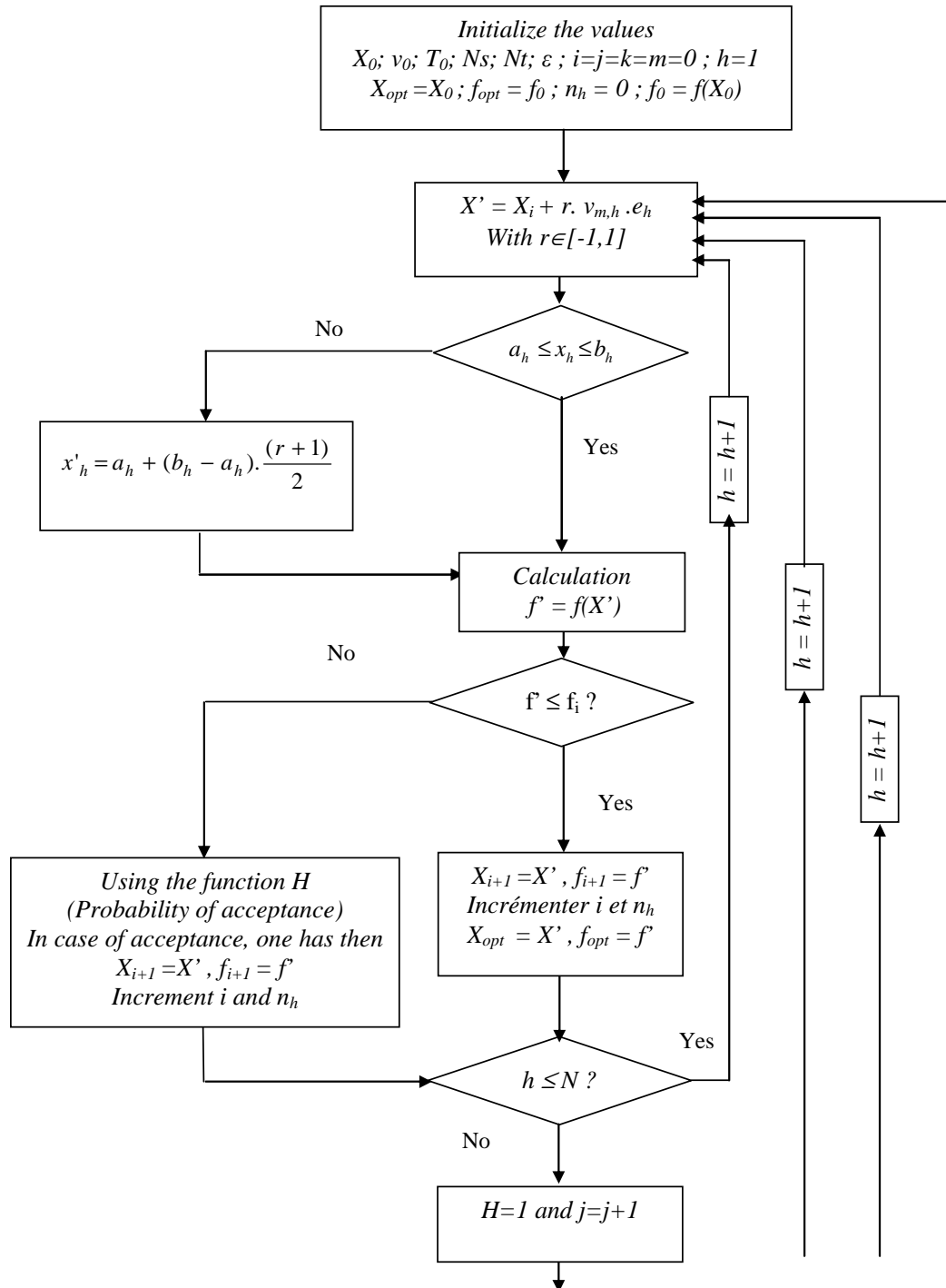
When the temperature is null, the probability of transition becomes unit. If energy decreases at the time of the transformation, and that it is null in the opposite case: the algorithm of Metropolis is then identical to an algorithm of iterative improvement, in this case, one is likely to finish trapped in local minima. On the other hand, when the temperature is not null, the algorithm can choose points with a value of the higher function, which makes it possible to avoid the minima in favour of global minima good located in the workspace.

Simulated annealing algorithms are expected to arrive at a good solution only in a statistical sense as in principale an infinitely large number of iterations are necessary to attain the global minimum. In practice to be useful, an acceptable solution must be attained in a finite reasonable number of iterations. For this to be possible, the cooling schedule must be carefully chosen so that the temperature falls only as fast as is compatible with maintaining a quasi equilibrium, otherwise the algorithm will lock in a secondary minimum.

Various cooling schedules have been experimented with (step by step, linear, geometric and exponential) and, as expected, it is important to cool slowly, particularly at low temperatures. Finally, for the tests described here, the modified exponential cooling schedule recommended by Rees Ball [13] is adopted. However, if a modified exponential scheduling is chosen, almost all process running give slightly different results in term of energy and weight values. This means that the resulting configuration is stable and close to the optimal one.

We used for the synthesis of our radiation pattern the simulated annealing algorithm presented by Corona [14]. This algorithm was tested by various authors and was compared with other techniques like the simplex or gradient conjugate known of

the functions comprising local minima. It proved that it always found the global minima which are not the case of the other methods. The algorithm is very simple and is presented in the following general form as shown in Fig. 3.



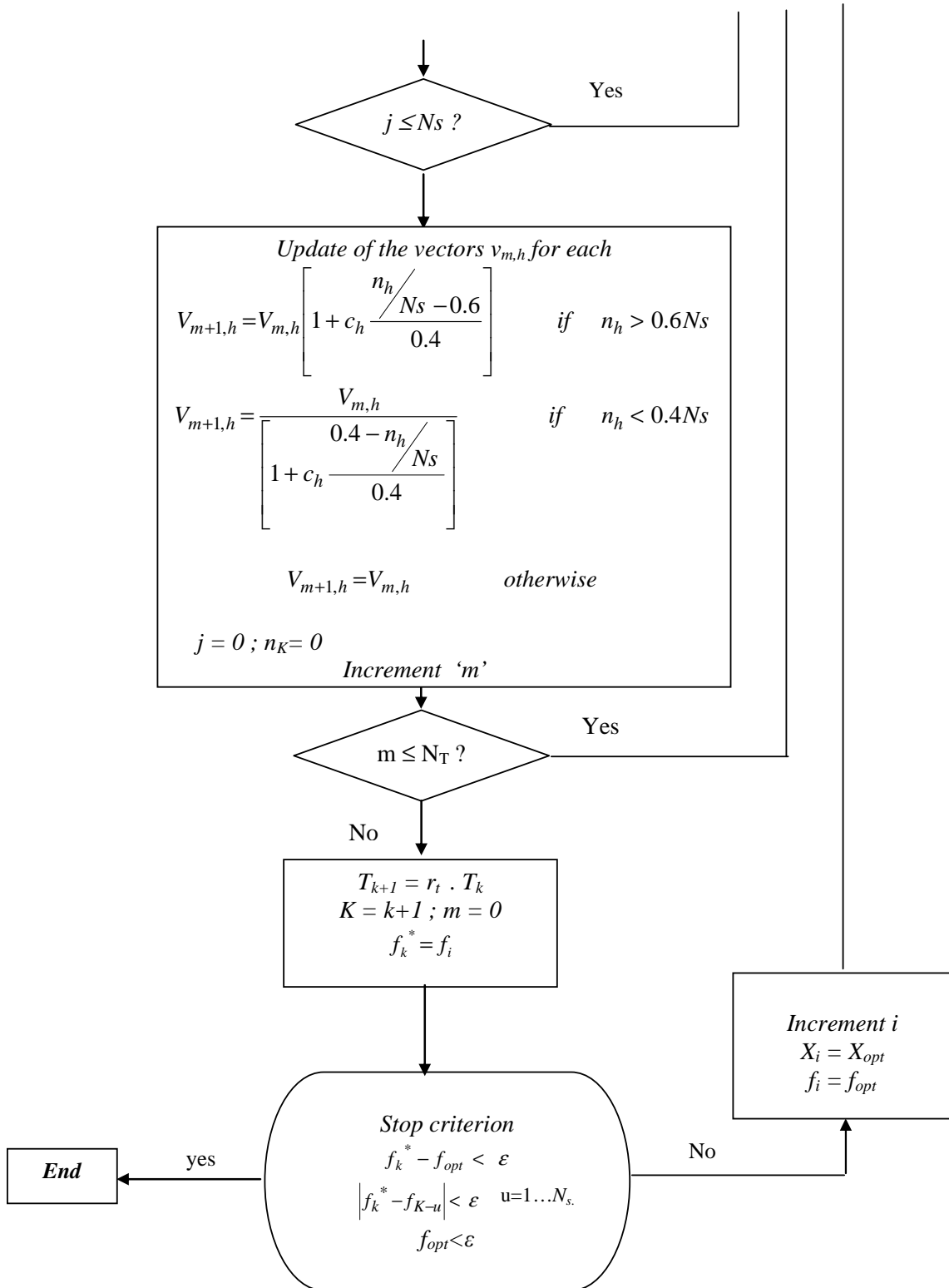


Figure 3: Simulated annealing flow chart.

Synthesis Results

In order to test performances of the proposed approach, we considered circular array with only one crown of 8 elements uniformly spaced at 0.5λ . The shape pattern is specified by an undulation domaine UD_{lim} of -5 dB, for a maximum width of principal beam is of 30° and a minimal width is of 18° , the maximum side lobes level is of -40 dB. The synthesized radiation pattern is shown in Fig. 4.

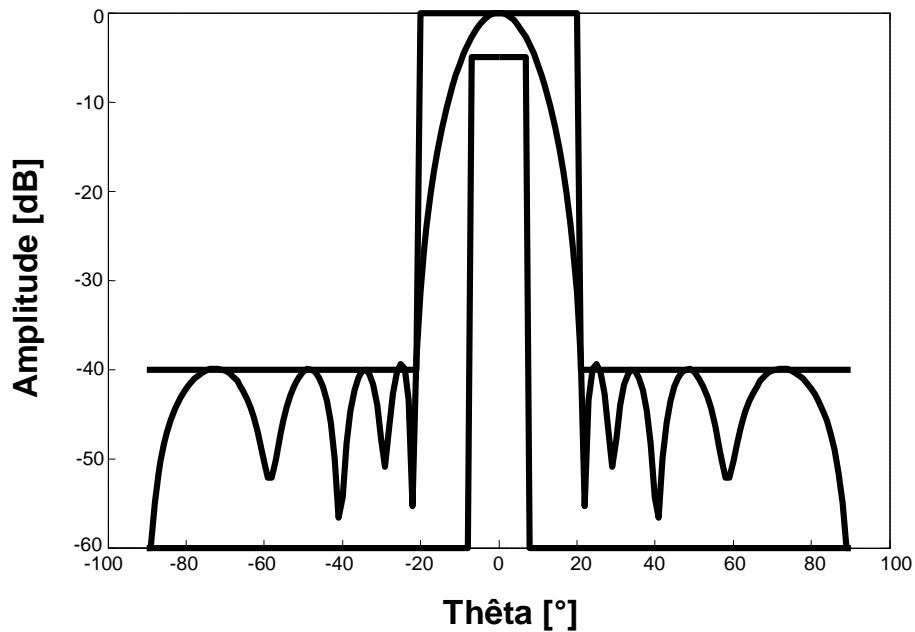


Figure 4: Optimization results of a circular array with one crown (N=8).

Notice that the synthesized radiation pattern is contained within the limits imposed by the desired shape pattern. Most of the power is concentrated around the angle $\theta = 0^\circ$. The main lobe is more directing than that of the linear array and the side lobes maximum is of -40 dB, which remains in agreement with the requirements.

A plot of the error evolution versus iterations is shown in Fig. 5 and Fig. 6 gives the feeding normalized amplitude of the sources.

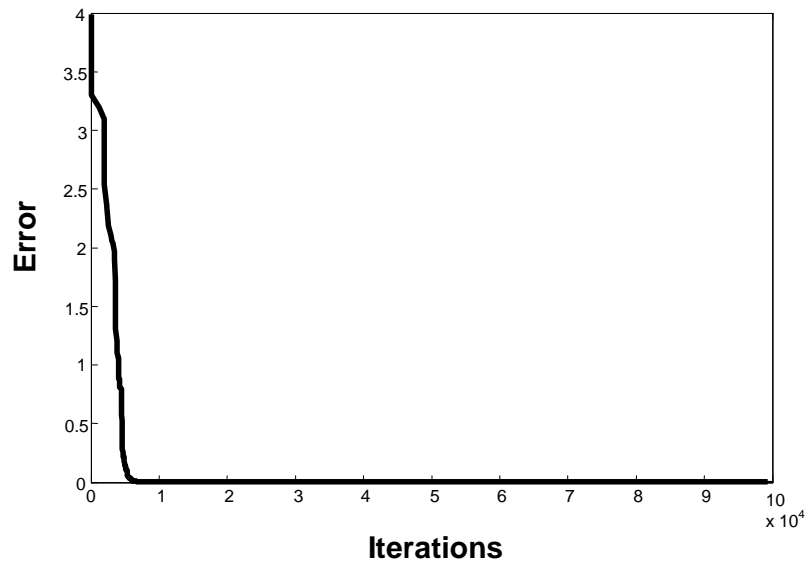


Figure 5: Error versus iterations.

According to the figure above, one notice that the algorithm converges at the end of 11×10^3 iterations.

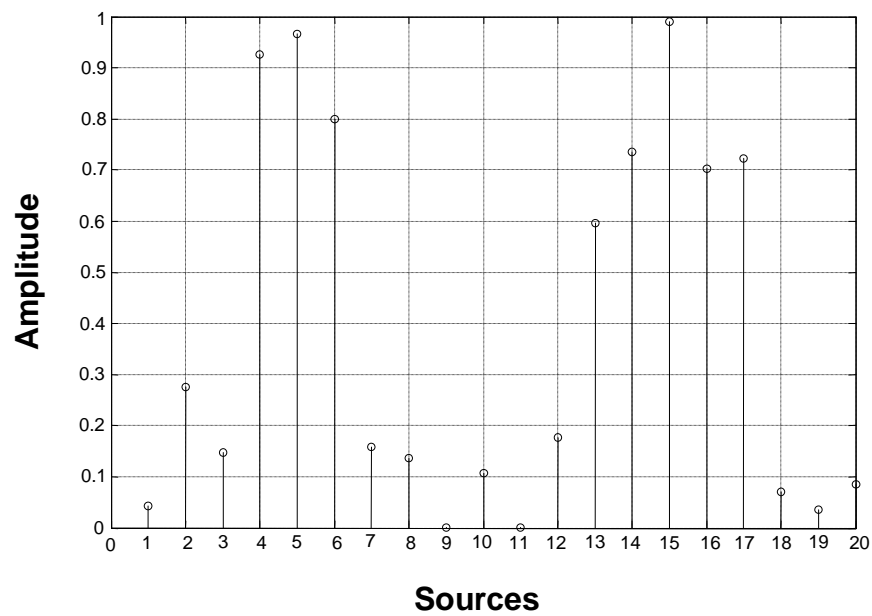


Figure 6: Feeding normalized amplitudes.

On Fig. 7, we show the synthesized radiation pattern of the a circular array with four crowns of 8 ($N=32$) elements each one.

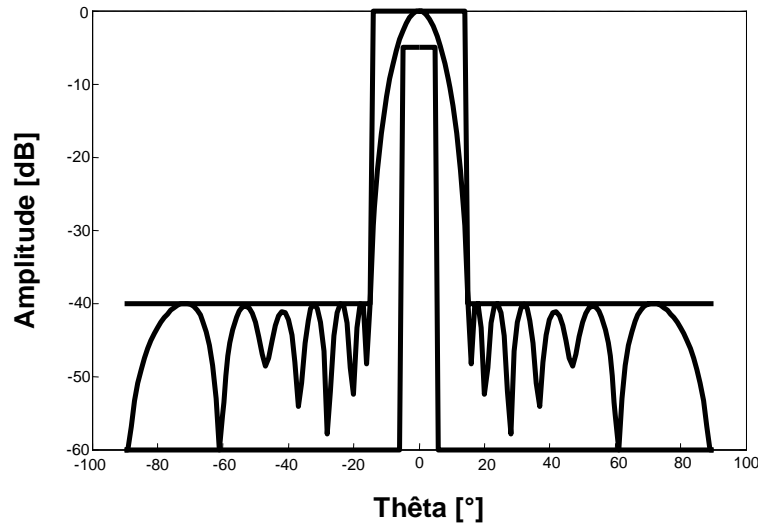


Figure 7: Optimization results of a circular array with four crowns ($N=32$).

Notice that a perfect symmetrical radiation pattern compared to the reference direction $\theta = 0^\circ$ is obtained. The synthesized pattern is contained in the desired shape. Good results was obtained for the side lobes levels where the more dominating is of -40 dB and the maximum tolerable value was fixed at -40 dB.

A plot of the error evolution versus iterations is shown in Fig. 8 and Fig. 9 gives the feeding normalized amplitude of the sources.

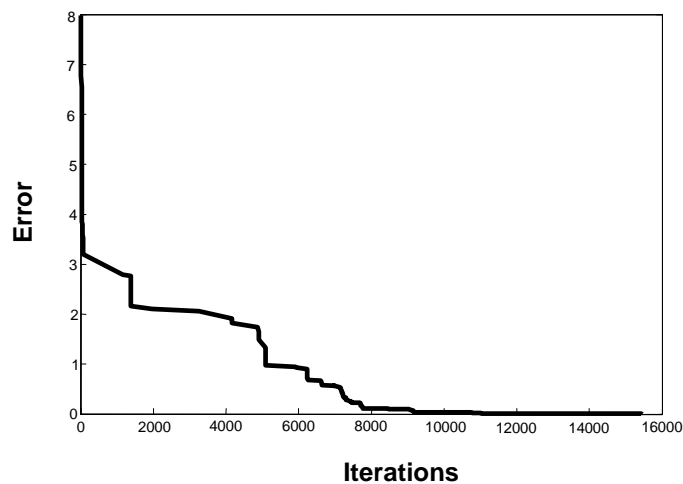


Figure 8: Error versus iterations.

According to the figure above, one notice that the algorithm converges at the end of 11×10^3 iterations.

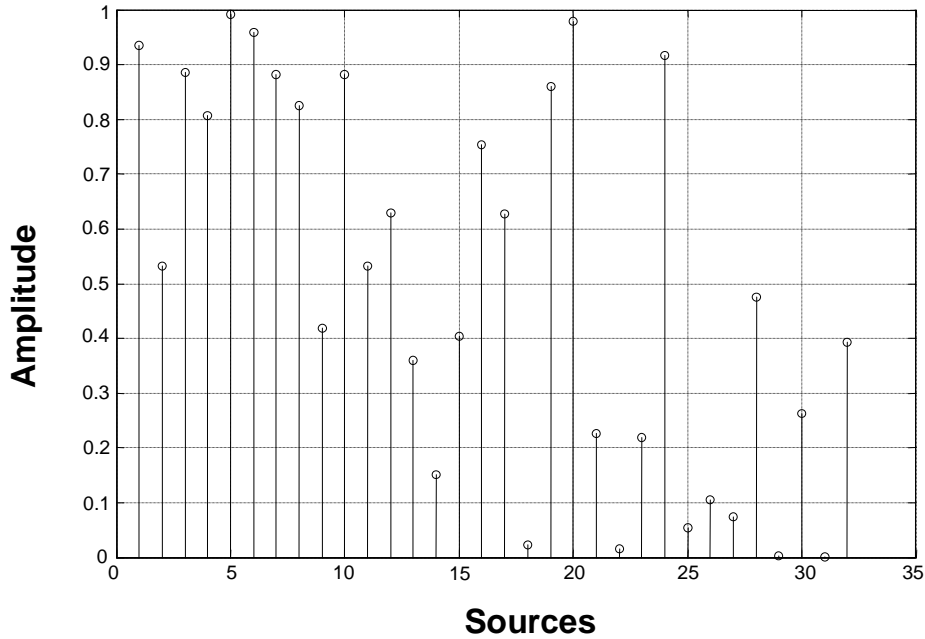


Figure 9: Feeding normalized amplitudes.

Conclusion

In this paper, we developed a global optimization algorithm of circular array of printed antennas based on the simulated annealing method by ordering the amplitude of excitation of each element of the array.

The two cases of arrays that we treated, using a synthesis technique based on the simulated annealing algorithm, substantiate that the application of such an heuristic algorithm achieved the goals of a most rigorous and global approach towards the best solutions. Such solutions remain difficult to achieve using calculus-based on deterministic methods which are too rigid and limited in search space by the local optima difficulties. Moreover, this algorithm is free from all restrictions associated to the integral calculus, derivatives, matrix algebra, discontinuities, etc...

The obtained results are very interesting of share their variety, their general information in the direction of reduction of the side lobes level. This method remains effective and robust towards badly conditioned problems, in particular when the solutions space he comprises discontinuities or constraints on the parameters and especially a great number of local minima. However, the choice of the cost function remains delicate, because the latter represents the key parameter of convergence towards an optimal solution.

References

- [1] Tillman JD. Theory and design of circular antenna arrays. The university of tennessee Experiment station 1966.
- [2] Mailloux RJ. Phased array antenna handbook. Artech House 1994.
- [3] Muorino A, Trucco CS. Reggazoni. Synthesis of uniquely Spaced arrays by simulated annealing. *IEEE Trans Antenna Propag* 1996;44: 119–1.
- [4] Morris D. Simulated Annealing Applied to the Misell Algorithm for Phase Retrieval. *IEE Proc-Microw Antenna Propag* 1996;143:298–8.
- [5] Washington G, Yoon HS, Angelino M, Theunissen WH. Design, Modeling, and Optimization of Mechanically Reconfigurable Aperture Antennas. *IEEE Trans Antenna Propag* 2002;50: 628–5.
- [6] Coleman CM, Rothwell EJ, Ross JE. Investigation of Simulated Annealing, Ant-Colony Optimization, and Genetic Algorithms for Self-Structuring Antennas. *IEEE Trans Antenna Propag* 2004;52: 1007–4.
- [7] Balanis CA. *Antenna Theory Analysis and Design*, 2nd ed., United States of America. John Wiley: 1997.
- [8] Bendimerad FT, Cambiaggio E, Papiernik. A. Synthesis of Uniformal Excited Non-periodic Antenna Arrays: Application to Microstrip Antenna. *Proc. IEEE Antennas and Propaga Society International Symposium* 1988;2:462 - 6.
- [9] Ribero JM, Staraj R, Damiano JP. Analytical models for fast analysis and synthesis of various printed antennas. *Antennas and associated systems for mobil satellite communication* 1997; 508.
- [10] Abri M, Boukli-hacene N, Bendimerad FT. Application du recuit simulé à la synthèse d'antennes en réseau constituées d'éléments annulaires imprimés. *Annales des Télécommunications* 2005 ;60 :1420-12.
- [11] Kirkpatrick S, Gelliatt CD, Vecchi MP. Optimization by simulated annealing. *Science* 1983;220;4598;372 – 7.
- [12] Girard T. Réseaux d'antennes imprimées sur des surfaces conformes. Thèse de doctorat, Université de nice-Sophia Antipolis 1999.
- [13] Rees S. Ball RC. Criteria for an optimum simulated annealing schedule for problems of the travelling salesman type. *J. Phy. A.:Math. Gen.* 1987;20:1239.
- [14] Corana A, Marchesi M, Martini C, Ridella S. Minimizing multimodal functions of continuous variables with the simulated annealing. *ACM transactions on mathematical software* 1987;13;3;262-9.

Phase-Only Planar Antenna Array Synthesis with Fuzzy Genetic Algorithms

Boufeldja Kadri¹, Miloud Boussahla², Fethi Tarik Bendimerad²

¹ Bechar University, Electronic Institute
P.O.Box 417, 08000, Bechar, Algeria

² Abou-Bakr Belkaid University, Engineering Sciences Faculty, Telecommunications Laboratory
P.O.Box 230, Tlemcen, Algeria

Abstract

This paper describes a new method for the synthesis of planar antenna arrays using fuzzy genetic algorithms (FGAs) by optimizing phase excitation coefficients to best meet a desired radiation pattern. We present the application of a rigorous optimization technique based on fuzzy genetic algorithms (FGAs), the optimizing algorithm is obtained by adjusting control parameters of a standard version of genetic algorithm (SGAs) using a fuzzy controller (FLC) depending on the best individual fitness and the population diversity measurements (PDM).

The presented optimization algorithms were previously checked on specific mathematical test function and show their superior capabilities with respect to the standard version (SGAs).

A planar array with rectangular cells using a probe feed is considered. Included example using FGA demonstrates the good agreement between the desired and calculated radiation patterns than those obtained by a SGA.

Keywords: fuzzy genetic algorithms, planar array, synthesis, population diversity measurements, fuzzy controller.

1. Introduction

Planar antenna arrays are fundamental components of radar and wireless communication systems [1]. Their performance heavily influences the overall system's efficiency and suitable design methods are necessary.

The phase-only methods are of particular interest in antenna array synthesis as phase shifters are used to control the direction of the main beam. These methods include in general nonlinear optimization algorithms.

The genetic algorithms (GAs) have been widely used in electromagnetic problems optimization, and particularly for the synthesis of antenna arrays. They have proved to be a useful and powerful alternative to traditional optimization techniques [2-7] when handling with

multidimensional, multimodal optimization problems and their success are related to their versatility, robustness and their ability to optimize non differentiable cost function [2-7].

However, GA has also some demerits, such as poor local searching, premature converging as well as slow convergence speed. Adaptive genetic algorithms (AGAs) have been developed to overcome these problems, where their control parameters are adjusted according to the variation of the environment in which the GAs are run. We introduce the well-known performances of the fuzzy set theory to adjust control parameters of GAs depending on current performance measures of GAs such as : maximum, average, minimum fitness and on the diversity of the population(PD).

We present in this paper the synthesis of the complex radiation pattern of a planar antenna array with probe feed by only optimizing the phase excitation coefficients, the desired radiation pattern is specified by a narrow beam pattern with a beam width of 8 degrees and a maximum side lobe levels of -20DB pointed at 10°.

Section 2 describes the fuzzy genetic algorithms (FGAs), the design of a fuzzy controller is discussed to adjust crossover and mutation probabilities according to the population diversity measurements and the best fitness individual. Section 3 shows the synthesis problem of a planar antenna array with rectangular cells using FGAs by optimization of the phase excitation coefficients.

Numerical results for a planar array using both the SGAs and FGAs are presented in section 4, to compare the performances obtained while introducing fuzzy techniques in GAs. Finally, some conclusions are drawn in section 5.

2. Fuzzy Genetic Algorithms

The GAs behavior is determined by the exploitation and exploration relationship kept throughout the GA run. This balance between the utilization of the whole solution space

and the detailed searching of some parts can be adapted to change of GA operators setting (selection, crossover and mutation). So, different genetic operators or control parameters values maybe necessary during the course of a run for inducing an optimal exploration/exploitation balance. For these reasons, adaptive GAs have been built that dynamically adjust selected control parameters or genetic operators during the course of evolving a solution [8] [9].

One way for designing AGAs involves the application of fuzzy logic controller (FLCs) [10-12] for adjusting GA control parameters.

The main idea of adaptive GAs based on fuzzy controllers FLCs is to use a FLC whose inputs are any combination of GA performances measures or current control parameters and whose outputs are GA control parameters. Current performance measures of the GA are sent to the FLC, which computes the new control parameters values that will be used by the GA as demonstrated by the flowchart shown in figure 1.

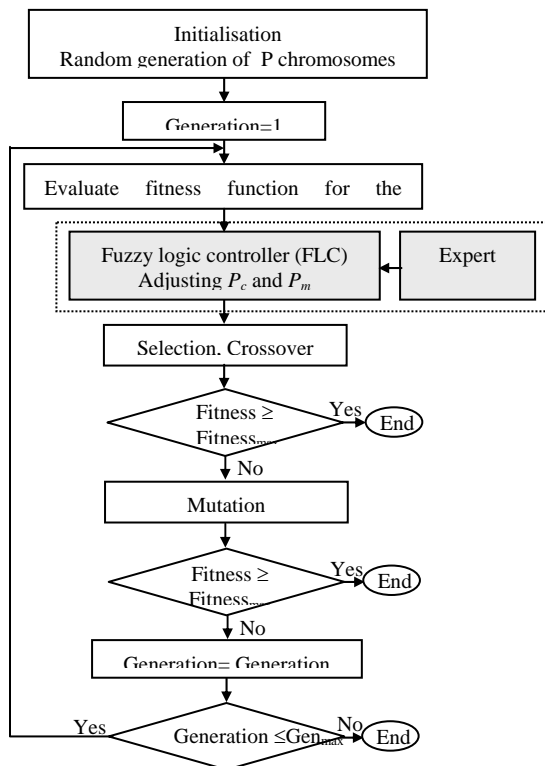


Fig. 1 Flowchart of the fuzzy genetic algorithms (FGAs).

FLC's inputs should be robust measures that describe GA behavior and the effects of genetic setting parameters and genetic operators, some possible inputs were cited in [9][10]: diversity measures, maximum, average, minimum fitness.

FLC's outputs indicate the values of control parameters or changes in these parameters, the following outputs were

reported in [9] [10]: mutation probability (p_m), crossover probability (p_c), population size ... etc.

We have choose for FLC's outputs the probabilities of crossover p_c and mutation p_m to realize the twin goals of maintaining diversity in population and sustaining the convergence capacity of the GA[13] [14].

The significance of p_c and p_m in controlling GA performance has long been acknowledged in GA research [6] [7]. Several studies, both empirical [15] [16] and theoretical [17] have been devoted to identify optimal parameter settings for GAs. The crossover probability p_c controls the rate at which solutions are subjected to crossover. The higher the value of p_c , the quicker are the new solutions introduced into the population. As p_c increases, however, solutions can be disrupted faster than selection can exploit them.

Mutation is only a secondary operator to restore genetic material choice. Nevertheless the choice of p_m is critical to GA performance and has been emphasized in Dejong's work [18]. Large value of p_m transforms GA into a purely random search algorithm, while some mutation is required to prevent the premature convergence of the GA to suboptimal solutions.

The FLC design takes into account the PDM and a performance measure of GAs, in this paper the FLC has three inputs (D_{gw} , \bar{f}/f_{max} and Number) and two outputs (p_c and p_m) as indicated in the figure 2.

Where:

\bar{f} : is the average fitness of the current population.

f_{max} : is the fitness of the optimal individual.

D_{gw} : is the gene inner diversity.

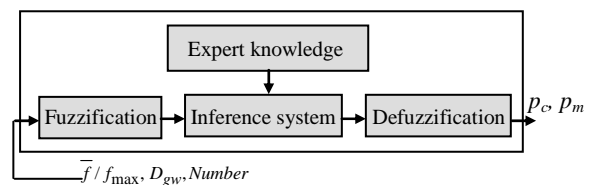


Fig. 2 Structure of the fuzzy logic controller FLC.

Let us consider a given population with M individuals (p_1, \dots, p_M) where each individual is represented by a binary string of l bits, the PDM can be described by means of the gene inner diversity given by equation 1:

$$D_{gw} = \bar{\delta}_1 = \frac{1}{M.l} \sum_{i=1}^M \sum_{j=1}^l \left(p_i^j - \bar{g}^j \right)^2 \quad (1)$$

Where

p_i^j : represents the j^{th} bit gene value of the i^{th} individual string.

\bar{g}^j : is the gene average calculated by equation 2.

$$\bar{g}^j = \frac{1}{M} \cdot \sum_{i=1}^M p_i^j \quad (2)$$

D_{gw} represents the genetic drift degree and evolution ability of current population. \bar{f}/f_{\max} is used to judge whether the current PD is useful [12], if it's near to 1, convergence has been reached, whereas if it's near to 0, the population shows a high level of diversity[10]. Number is used to record the frequency of the largest fitness value that is not changed.

The input variables D_{gw} , \bar{f}/f_{\max} and Number to be included respectively in the ranges : [0 , 0.25], [0 , 1] and [0 , 30].

Once the inputs and outputs of the FLC are defined, we must drive the membership functions and the fuzzy rules. More details about the design of FLC are given in [12].

3. Synthesis of Planar Antenna Arrays

We develop in this paper a synthesis of planar antenna array with probe feed using the FGAs discussed in the previous section.

Let us consider a planar antenna array constituted of $M \times N$ equally spaced rectangular antenna arranged in a regular rectangular array in the x-y plane, with an inter-element spacing of $d = dx = dy = \lambda/2$ as indicated by figure 3, and whose outputs are added together to provided a single output. Mathematically, the normalized array far-field pattern is given by:

$$F_s(\theta, \phi) = \frac{f(\theta, \phi)}{F_{s\max}} \cdot \sum_{m=1}^M \sum_{n=1}^N I_{mn} \cdot e^{j(m-1)k_0 \cdot \sin\theta \cdot \cos\phi \cdot dx + j\psi_{mn}} \cdot e^{j(n-1)k_0 \cdot \sin\theta \cdot \sin\phi \cdot dy} \quad (3)$$

Where

$f(\theta, \phi)$: Represents the radiation pattern of an element.

I_{mn} : Amplitude coefficient at element (m, n) .

ψ_{mn} : Phase coefficient at element (m, n) .

k_0 : Wave number.

If we consider an array with separable distribution, then the array factor is the product of two linear arrays associated with the row and column direction of this planar, which can be expressed in the form (4):

$$F_s(\theta, \phi) = \frac{f(\theta, \phi)}{F_{s\max}} \cdot \sum_{m=1}^M I_m \cdot e^{j(m-1)k_0 \cdot \sin\theta \cdot \cos\phi \cdot dx + j\psi_{mn}} \cdot \sum_{n=1}^N I_n \cdot e^{j(n-1)k_0 \cdot \sin\theta \cdot \sin\phi \cdot dy} \quad (4)$$

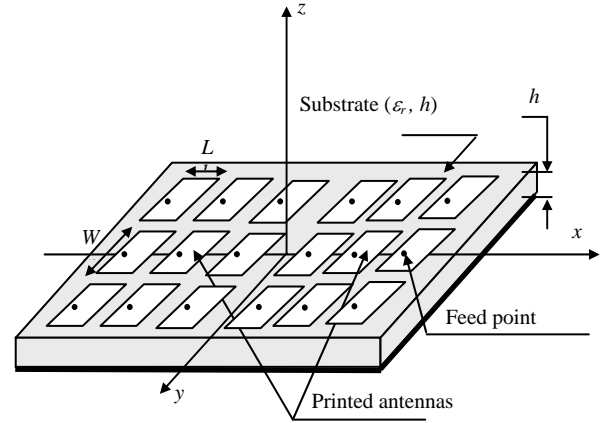


Fig. 3 Planar antennas array fed by coax.

We use the FGAs to find the complex excitation coefficient vector

$$A = \left[\psi_{x1}, \psi_{x2}, \dots, \psi_{x\frac{M}{2}}, \psi_{y1}, \psi_{y2}, \dots, \psi_{y\frac{N}{2}} \right] \quad \text{so the}$$

radiation pattern produced satisfy the desired radiation pattern specified by the pattern model as illustrated in figure 4. This pattern has a narrow beam with -20DB sidelobes. The pattern is normalized to the peak value at 10 degrees and must have a 3DB beamwidth of at least 8 degrees. The -20DB sidelobe level must be met beginning at 0 and 20 degrees and extending to ± 90 degrees. The sidelobes in this case are defined relative to the peak of beam at 10 degrees. The specifications are illustrated in figure 4.

We have choose a suitable fitness function that can guide the SGAs and FGAs optimization toward a solution that meets the desired radiation pattern as mentioned in [1]. Equations 5-7 describe the appropriate fitness function.

$$d_{av} = \frac{1}{2S+1} \sum_{i=-S}^S d_i \quad (5)$$

$$Sll_{\max} = \min_{\forall i \in \text{Sidelobes}} (|d_{av} - d_i|) \quad (6)$$

$$\text{fitness} = d_{av} + w_1 Sll_{\max} \quad (7)$$

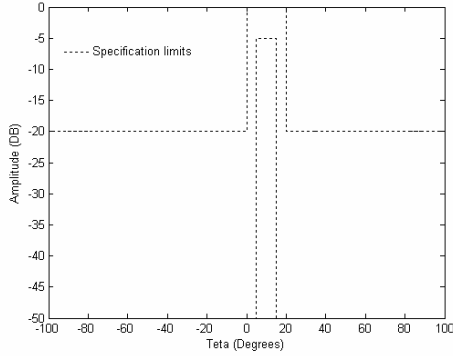


Fig. 4 Plot of the desired pattern specification (for 10° main beam).

Where it is assumed that a number of samples of the pattern, d_i in dB, are taken in the beam region and the sidelobe region and that the number of samples in the beam region is equal to $2S+1$. An arbitrary weight w_l is used. The goal of function (7) is to maximize the difference between the average value in the beam and the highest sidelobe.

First we have to find a relationship between the GAs and the array. In the case of a coded GA, each element of the array is represented by a string of bits which gives the complex excitation of the element; hence each element is characterized by its phase excitations. This relationship is shown in table 1.

Table 1: The relationship between elements of GAs and arrays.

Genetic parameters	Antennas array
Gene	Bits chain(string): (phase)
Chromosome	One element of array
Individual	One array
Population	Several arrays

4. Numerical Results

In our simulation, we have used a population size of 40 for GAs. Roulette strategy for “selection” one-point crossover and mutation to flip bits. For the SGAs, we have used value of $p_c=0.71$ and $p_m=0.02$, for the FGAs, p_c and p_m are determined according to FLC presented previously.

We have chosen for simplification a symmetrical array, whose elements are located symmetrically on x-y plan, and adopted an antisymmetrical phases for elements, which can be resumed by equation (7):

$$\begin{cases} x_i = -x_{-i}, \psi_i = -\psi_{-i} \\ y_j = -y_{-j}, \psi_j = -\psi_{-j} \\ \text{for } i = 1, \dots, N/2, \text{ for } j = 1, \dots, M/2 \end{cases} \quad (8)$$

We have adopted a desired radiation pattern specified by a narrow beam pointed at 10 degrees with a sidelobe level of -20dB. Figures 5 to 8 show the synthesis result of a probe-fed planar array constituted by 8x16 half wavelength spaced rectangular microstrip antennas with 0.906cm width and 1.186cm long working at the frequency of 10GHz.

In figure 5 we present the result of planar array optimization by phase excitation coefficients using both SGAs and FGAs. It is clearly seen that the radiation pattern obtained by FGAs meet better the desired pattern than the obtained by SGAs. The sidelobe level obtained by FGAs optimization (-26DB) are much better than in the case of SGAs (-20DB).

From figure 6, the speed approaching the global optimal of FGA is much quickly than that of SGA, and the fitness values of the best individuals of FGA are almost higher than that of SGA in every population. For each generation the probabilities p_c and p_m are adjusted according to the response of the fuzzy controller, and shown in the figures 7 and 8.

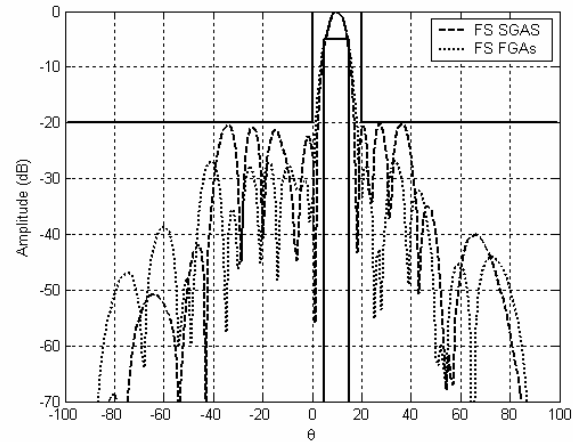


Fig. 5 Result of a planar array synthesis with 8x16 rectangular microstrip antennas applying both SGAs and FGAs.

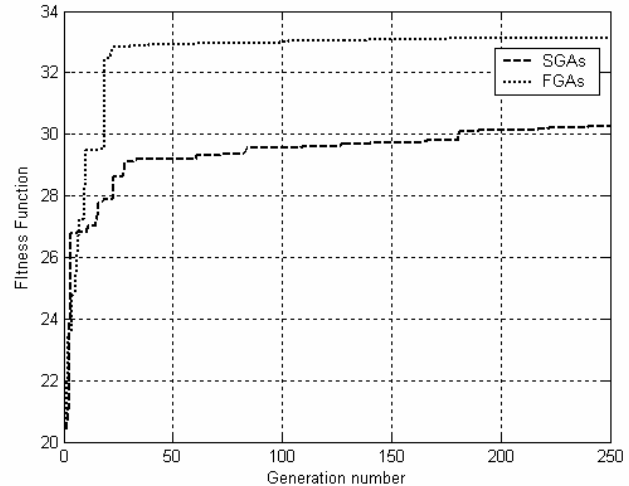


Fig. 6 Comparison between fitness functions obtained by the two algorithms SGAs and FGAs.

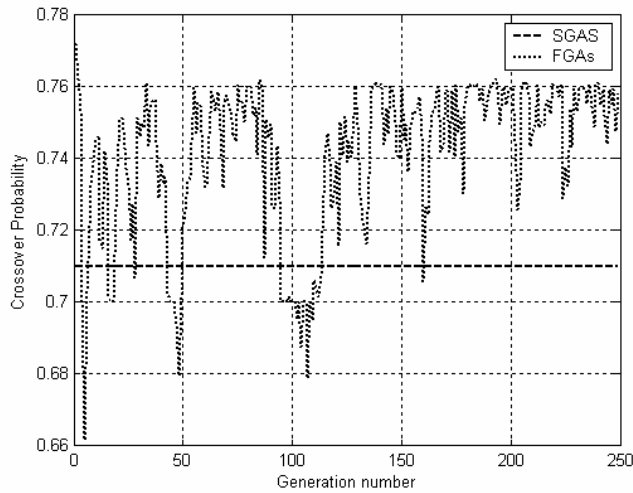


Fig. 7 Adjusting p_c during GAs run.

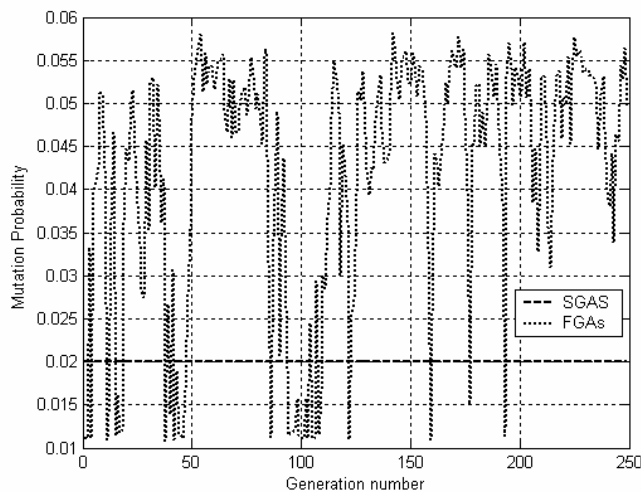


Fig. 8 Adjusting p_m during GAs run.

5. Conclusions

A rigorous method for the synthesis of planar antenna array using AGAs integrating a FLC by optimizing only phase excitation coefficients has been presented. The GAs behavior is strongly determined by the balance between exploiting what already works best and exploring possibilities that might eventually evolve into something even better.

The balance between these characteristics (exploration and exploitation) of the GAs is dictated by the values of p_c and p_m . We have adopted the variation of p_c and p_m according to the response obtained by a FLC which

depends on the PDM and a measure of the convergence by means of the ratio between the best fitness and average fitness. With the approach of adaptive probabilities of crossover and mutation, we also provide a solution to the problem of choosing the optimal values of the probabilities of crossover and mutation for the GA.

From the simulating results, it has been shown that the speed approaching the global optimal of FGA is much quickly than that of SGA, and the fitness values of the best individuals of FGA are almost higher than that of SGA in every population.

References

- [1] R. L. Haupt, J. M. Johnson, "Dynamic Phase-Only Array Beam Control using a Genetic Algorithm", 1st NASA/DOD Workshop on Evolvable Hardware 217-224, EH'99, July 19-21, Pasadena, CA, USA
- [2] R. L. Haupt, "An Introduction to Genetic Algorithms for Electromagnetics", IEEE Antenna and propagation Magazine, Vol. 37, pp. 7-15, 1995.
- [3] S. A. Mitlineos, C. A. Papagianni, G., I. Verikaki, C. N. Capsalis, "Design of Switched Beam Planar Arrays Using the Method of Genetic Algorithms", Progress In Electromagnetics Research, PIER 46, 105-126, 2004.
- [4] D. Marcano, F. Duran, "Synthesis of Antenna Arrays Using Genetic Algorithms", IEEE Antenna and propagation Magazine, Vol. 42, NO. 3, June 2000.
- [5] M. Donelli, S. Coarsi F. De Natale, M. Pastorino, A. Massa, "Linear Antenna Synthesis with Hybrid Genetic Algorithm", Progress in Electromagnetics Research, PIER 49, 1-22, 2004.
- [6] D. E. Goldberg, "Genetic Algorithms in Search, Optimization and Machine Learning", Reading, MA: Addison Wesley, 1989.
- [7] K. A. Dejong, "Genetic Algorithms: A 10 year perspective", in Proceedings of an International Conference of Genetic Algorithms and Their Applications, (J Greffentette, editor), Pittsburgh, July 24-26, 1985, PP. 169-177.
- [8] M. Srinivas, L. M. Patnaik, "Adaptive Probabilities of Crossover and Mutation in Genetic Algorithms", IEEE Trans. Syst. Man and Cybernetics, 1994, 24(4): 656-667.
- [9] F. Herrera, M. Lozano, "Adaptive Genetic Operators Based On Coevolution with Fuzzy Behaviors", IEEE Transaction on Evolutionary Computation, Vol. 5, NO. 2, 2001.
- [10] M. A. Lee, H. Takagi, "Dynamic Control of Genetic Algorithms Using Fuzzy Logic Techniques", International Conference on Genetic algorithms ICGA'93, Urbana-Champaign, pp. 76-83, 1993
- [11] B. Kadri, F.T. Bendimerad, "Fuzzy Genetic Algorithms for The Synthesis of Unequally Spaced Microstrip Antennas Arrays", European Conference on Antennas And Propagation EUCAP2006, Nice, 6-10 November 2006, (ESA SP-626, October 2006).
- [12] K. Wang, "A New Fuzzy Genetic Algorithm Based on Population Diversity", International Symposium on Computational Intelligence in Robotics and Automation, pp. 108-112, July 29 August 1, 2001, Alberta, Canada.

- [13] Xiagofeng Qi, Francesco Palmieri, "Theoretical Analysis of Evolutionary Algorithms with an Infinite Population Size in Continuous Space, Part II: Analysis of the Diversification Role of Crossover", IEEE Trans on Neural Networks, 1994, 5(1)
- [14] Z. Liu, J. Zhou, Z. Wei, H. Lv, L. Tao, "A Study on Novel Genetic Algorithm with Sustaining Diversity", Proceeding of ICSP2000, 1650-1654.
- [15] J. J. Greffentette, "Optimization of Control Parameters for Genetic Algorithms", IEEE Trans. Syst. Man., and Cybernetics, Vol. SMC-16, No. 1, pp. 122-128, Jan/Feb, 1986.
- [16] J. D. Schaffer et, al., "A Study of Control Parameters Affecting online Performance of Genetic Algorithms for Function Optimization", Proc. Third Int. Conf. Genetic Algorithms, 1989, pp. 51-60.
- [17] J. Hesser, R. Manner, "Towards an Optimal Probability for Genetic Algorithms", Proceeding of the First Workshop, PPSN-I, pp. 23-32, 1990.
- [18] K. A. Dejong, "An Analysis of the Behavior of a Class of Genetic Adaptative Systems", Ph.D. Dissertation, University of Michigan, 1975.

Boufeldja Kadri was born in Bechar, Algeria, in 1972. He received the Majister degree in 1998, from the Abou Bekrbelkaid University in Tlemcen (Algeria). Since 1999, he joined the Electronic Institute in Bechar University (Algeria), where he is now an associate professor. His research interests include modelling and optimization of antenna array, heuristic algorithms.

Miloud Bousahla was born in Sidi BelAbbès, Algeria, in 1969. He received the Magistère diplomas in 1999 from Abou BekrBelkaid University in Tlemcen (Algeria). He is currently a Junior Lecturer in the Abou BekrBelkaid University. Also he is a Junior Researcher within the Telecommunications Laboratory. He works on design, analysis and synthesis of antenna and conformal antenna and their applications in communication and radar systems.

Fethi Tarik Bendimerad was born in Sidi BelAbbès, Algeria, in 1959, he received his Phd degree from the Sophia-Antipolis University in Nice (France), in 1989. He is currently a full professor at the Faculty of engineering at the Abou BekrBelkaid University in Tlemcen, (Algeria) and the Director of the Telecommunications Laboratory. His field of interest is antenna treatment and smart antenna.

A Log Periodic Series-Fed Antennas Array Design Using A Simple Transmission Line Model

M. Abri, F. T. Bendimerad, N. Boukli-Hacene and M. Bousahla

*Laboratoire de Télécommunications, Département de Télécommunications
Faculté des Sciences de l'Ingénieur, Université Abou-Bekr Belkaïd -Tlemcen
BP 230, Pôle Chetouane, 13000 Tlemcen- Algeria*

Abstract

In this paper, a transmission line model is used to design a series-fed log periodic antennas arrays over a band of frequencies for satellite communications. The transmission line model is simple, precise and allowing taking into account the whole geometrical, electrical and technological characteristics of the antennas arrays. To validate this last, the obtained simulation results are compared with those obtained by the moment's method (MoM). Using this transmission line approach the resonant frequency, input impedance, return loss can be determined simultaneously. Agreements between transmission line model data and the moment's methods results were achieved.

Key words: Log periodic antennas, antennas array, transmission line model, moment's method (Momentum).

Introduction

Modern technologies are directed towards the miniaturization of antennas while trying to keep the best performances, the printed antenna is designed to satisfy these needs, it is a conductive metal of particular form placed on a substrate finished by a ground plane, its miniature character makes it possible to integrate it easily in emission and reception systems. A printed antenna presents a weak band-width and gain, association in array of several printed antennas makes it possible to compensate the single antenna limitations characteristic and to improve their gain and radiation performances, although their design is difficult because of their electromagnetic structure complexity, these antenna have the advantage of being able to be manufactured in great quantity with very weak cost. One of the antennas disadvantages remains a narrow band-width.

The broad band systems interest is confirmed day after day. The telecommunication standards multiplication of the future terminals, the exploitation of the ultra high frequency in various fields requires the use of broad band antennas.

Various techniques have been proposed to improve the bandwidth operation of microstrip elements, such as using thicker substrates combined with very low dielectric constant materials, using parasitic elements [1]-[3], using impedance matching networks [4] and using two or more electromagnetically coupled patches on top of one another or stacked [5]-[7]. Another successful attempt to enhance the bandwidth of microstrip antenna was made by applying the log-periodic technique to design a microstrip array.

The antennas analysis requires a significant number of electromagnetic simulations. The antennas characterization need the use of software based on rigorous numerical methods like the integral equations solved by the moment's method. Such EM simulations are very expensive in CPU time and which increases dramatically with the unknown number resulting from discretization of the studied structure. Recently, fast algorithms models applied in electromagnetic have been reported in literature.

In the present work, an attempt was made to design a log-periodic printed antennas array (LPA) by the equivalent transmission line model which makes it possible to take in account the whole antennas geometrical, electrical characteristics of and their feed system.

Log periodic antennas formulation

The LPA have properties which reproduce periodically according to the logarithm of the frequency. They are made of radiating elements resulting from/to each other starting from a multiplication of their dimension by a factor τ .

The design of the wideband array was based on frequency-independent antenna principle which, when applied to a periodic structure, result in scaling of the dimensions from period to period so that the performance is periodic with the logarithm of frequency [8]- [9]. This principle was used to design each row of the microstrip linear array of Fig. 1. The patch length L , width W and spacing between two adjacent elements were related initially to the scale factor τ by:

$$\tau = \frac{L_{n+1}}{L_n} = \frac{W_{n+1}}{W_n} \quad (1)$$

The scale factor was chosen to overcome the disadvantage of the narrow band performance of microstrip patches. If one multiplies all dimensions of the array by with τ the element n become $n+1$ and the element $n+1$ become the element $n+2$. Consequently the array will have the same radiation properties at all the frequencies which are connected by the scaling factor τ .

$$f_1, f_2 = \tau \cdot f_1, f_3 = \tau^2 f_1, f_4 = \tau^3 f_1 \quad (2)$$

Where:

$$\ln \frac{f_2}{f_1} = \ln \tau; \ln \frac{f_3}{f_1} = 2 \ln \tau \tag{3}$$

Where:

l is the distance between two adjacent radiating element.

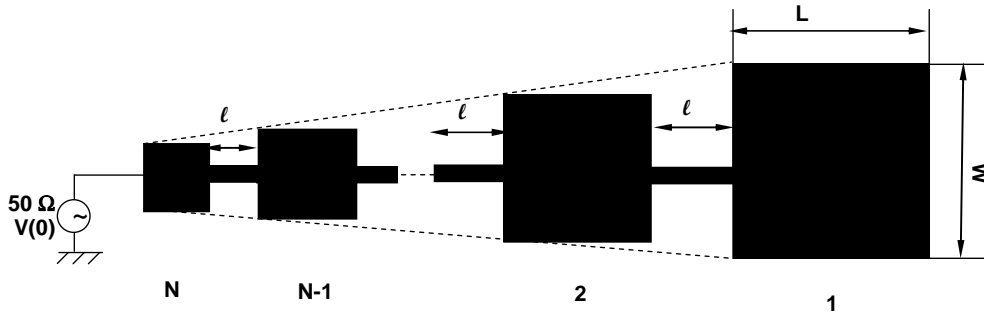


Figure 1: Log periodic antennas array architecture.

To calculate the input impedance of the printed antennas array, one supposes to exploit the electric model are equivalent of each radiating element to lead to a complete electric modelling of the entire array.

The LPA equivalent circuit is presented in the following Fig 2:

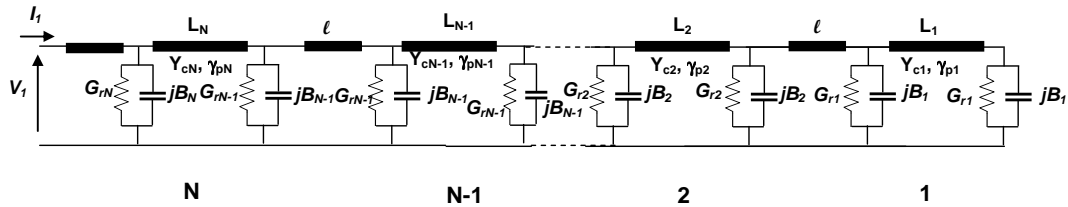


Figure 2: Equivalent circuit of the log periodic antennas array.

Antennas array operating in the band [6.2-8.2 GHz]

The antennas array is to be designed on RT/Duroid 5880 substrate which has a relative permittivity ϵ_r of 2.32, a dielectric thickness h of 1.588 mm, a loss tangent of about 0,002 and 0.05 mm conductor thickness. Log periodic array is designed to operate over the frequency range of 6.2 GHz to 8.2 GHz. Because the input impedance of a patch at its edges is usually too high for direct connection to the feeding line, whose standard impedance is 50 Ohm. A quarter wave transformer can be designed to achieve a satisfactory return loss at the resonant frequency. Using the

procedure mentioned above, a linear log-periodic array with nine elements was initially designed. The resonant frequencies and dimensions of each radiating element are listed in table 1. The scaling factor is $\tau=1.031$.

Table 1: Frequencies and radiating elements dimensions.

Element number	1	2	3	4	5	6	7	8	9
Frequency (GHz)	7.03	7.24	7.45	7.70	7.94	8.18	8.44	8.70	8.97
W=L (mm)	16.56	16.06	15.57	15.11	14.65	14.21	13.78	13.36	12.96

The antennas array architecture is shown in the figure below. The simulated input return loss of the antennas array is displayed for frequencies between 4.0 to 10.0 GHz in Fig. 3 (a).

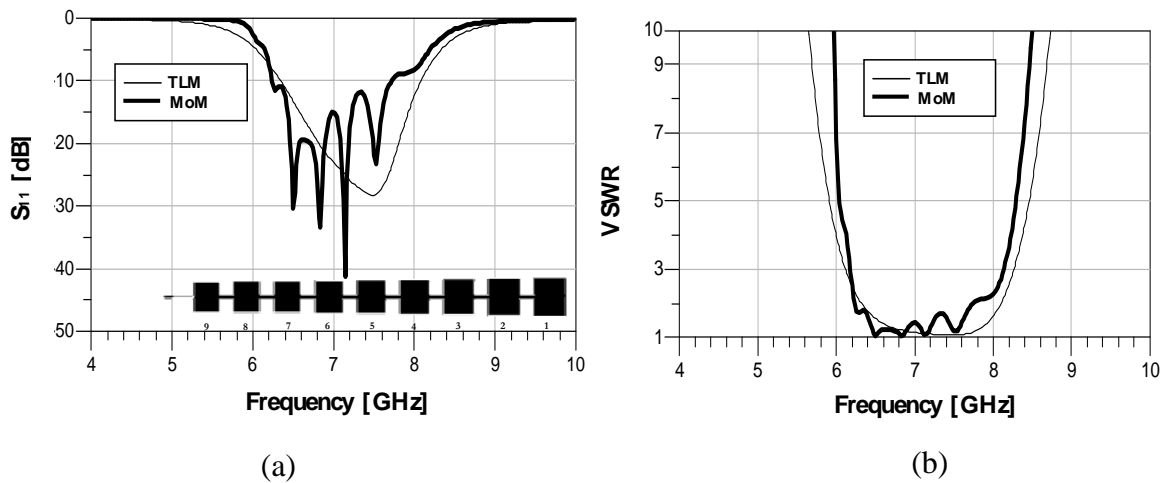


Figure 3: Log periodic antennas array.

(a) Computed return loss of the log periodic antennas array

(b) Computed VSWR

Let us note that the obtained band-width by the transmission line model is of about 1550 MHz and 1800 MHz by the moment's method. Notice according to the Fig. 3 (b), a good similarity between the two curves.

The impedance locus of the antennas array from 4.0 to 10.0 GHz is illustrated on Smith's chart in Fig. 4.

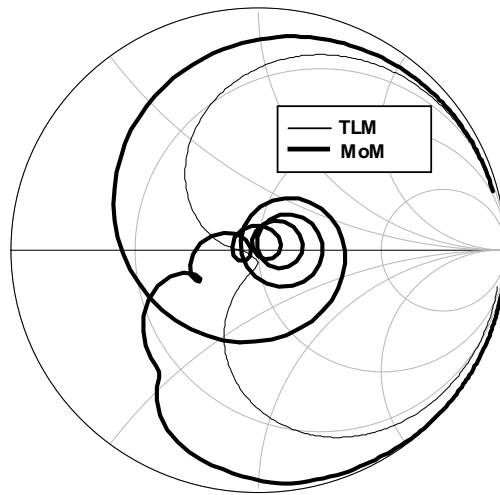


Figure 4: Smith's chart of the input impedance return losses. Frequency points given by start = 4.0 GHz, stop = 10.0 GHz.

The input impedance of the antenna has been calculated over a frequency range of 4.0- 10.0 GHz. It can be seen from Fig 4 that the comparison for the input impedance between transmission line model and the moment method results are in good agreement. Notice that the resonant frequency is very close to the axis of 50 Ohm.

Log periodic antennas array operating in the band [8.7-11.1 GHz]

The antennas array is to be designed on substrate which has a relative permittivity ϵ_r of 2.2, a dielectric thickness h of 1.588 mm, a loss tangent of about 0,002 and 0.05 mm conductor thickness. Using the transmission line model, the return loss, VSWR, input impedance are presented and resonant frequency is found to be in the band [8.7-11.1 GHz]. Because the input impedance of a patch at its edges is usually too high for direct connection to the feeding line, whose standard impedance is 50 Ohm. A quarter wave transformer can be designed to achieve a satisfactory return loss at the resonant frequency.

Nine radiating elements are used in this case. The resonant frequencies and dimensions of each radiating element are listed in table 2. The scaling factor is of about $\tau=1.04$.

Table 2: Frequencies and radiating elements dimensions.

Element number	1	2	3	4	5	6	7	8	9
Frequency (GHz)	8.52	8.86	9.21	9.58	9.96	10.35	10.77	11.20	11.65
W=L (mm)	13.66	13.13	12.62	12.14	11.67	11.22	10.78	10.37	9.97

The optimized antennas array layout is shown in the figure below. The simulated input return loss of the log periodic antennas array is displayed for frequencies between 6.0 to 12.0 GHz in Fig. 5 (a).

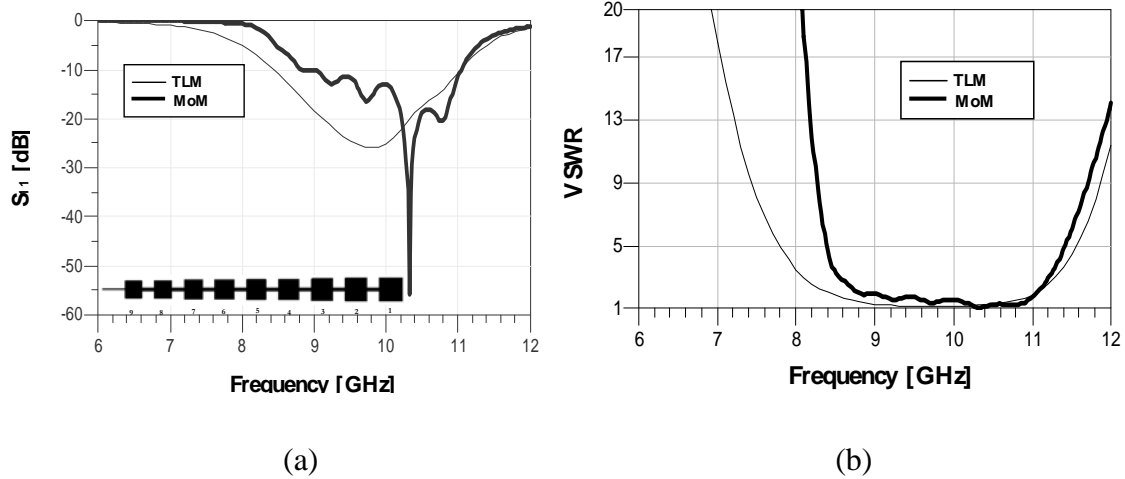


Figure 5: Log periodic antennas array.
 (a) computed return loss of the log periodic antennas array
 (b) computed VSWR

It is well observed that the resonance of the antennas array is correctly predicted to 10 GHz with a light shift by the moment's method. By calculating the band-widths one finds a width of 2600 MHz obtained by the transmission line model and 2200 MHz by the moment's method. The band-width ($S_{11} \leq -9.54$ dB) is obviously quite broad band. Notice according to Fig 5 (b) representing the computed VSWR that the two curves are almost identical. In the vicinity of the resonant frequency the VSWR is close to the unit which corresponds to an ideal matching.

The impedance locus of the antennas array from 6.0 to 12.0 GHz is illustrated on Smith's chart in Fig. 6.

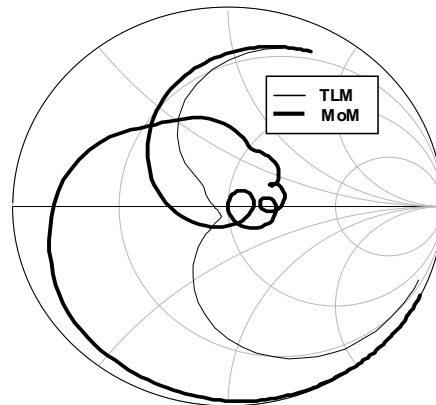


Figure 6: Smith's chart of the input impedance return losses. Frequency points given by start = 6.0 GHz, stop = 12.0 GHz.

Log periodic antennas array operating in the band [9.0–12.0 GHz]

In this section, other geometry is analyzed by using the method proposed in this paper. The permittivity and the substrate thickness are 2.32 and 1.588 mm respectively and the operation frequency band is [9.0-12.0 GHz]. A probe of 50 Ohm is employ to feed the log periodic antennas array.

A linear log-periodic array with 12 elements was initially designed. The resonant frequencies and dimensions of each radiating element are listed in table 3. The scaling factor is chosen to be $\tau=1.01$.

Table 3: Frequencies and radiating elements dimensions.

Element number	1	2	3	4	5	6	7	8	9	10	11	12
Frequency (GHz)	11.22	11.33	11.44	11.55	11.67	11.79	11.91	12.02	12.14	12.27	12.39	12.51
W=L (mm)	10.37	10.26	10.16	10.06	9.96	9.86	9.76	9.67	9.57	9.48	9.38	9.29

Figure bellow presents the mask layout for the log periodic antennas array operating in the band [9.0-12.0 GHz].

The simulated input return loss of the log periodic antennas array is displayed for frequencies between 8.0 to 13.0 GHz in Fig. 7 (a).

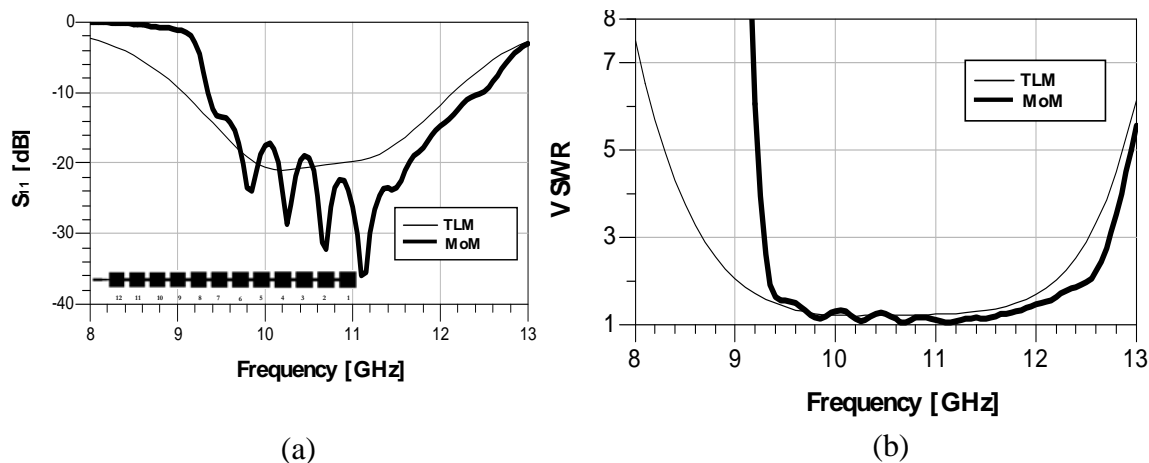


Figure 7: Log periodic antennas array
 (a) return loss of the log periodic antennas array
 (b) computed VSWR

Notice according to Fig. 7 (a) that both models are almost the same curves and that curve obtained by the moment’s method presents several peaks in the frequency band predicted in the table above. One obtained a band-width of 3200 MHz by the

transmission line model and 3050 MHz by the moment's method. It is a quite broad band what still proves the effectiveness of the log-periodicals structure in widening the band-width.

The simulated VSWR represented on the Fig. 7 (b) justified the obtained results by the computed return loss.

The impedance locus of the antennas array from 8.0 to 13.0 GHz is illustrated on Smith's chart in Fig. 8.

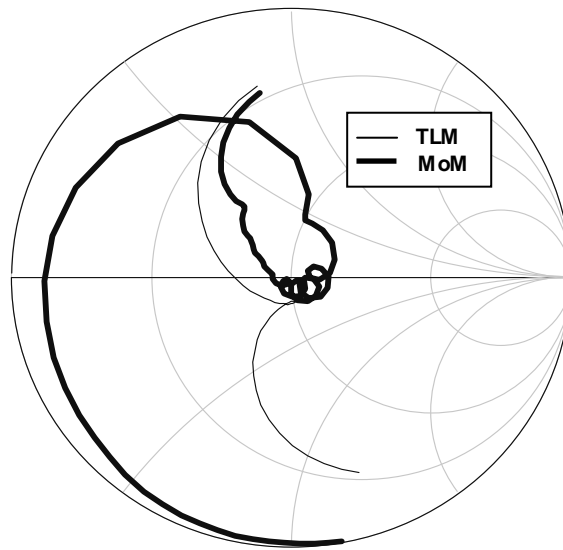


Figure 8: Smith's chart of the input impedance return losses. Frequency points given by start = 8.0 GHz, stop = 13.0 GHz.

It is observed that the two models curves passes by the axis of 50Ω and present both a null imaginary part witch mean a perfect matching at the resonant frequency.

Conclusion

In this paper several log periodic antennas arrays geometries to be employed in wide-band applications have been designed using a flexible and computation-efficient transmission line model. The results so far show that the transmission line model can be successfully used to predict the input characteristic of the antennas array over wide band frequencies. Even though the model is conceptually simple, it still produces accurate results in a relatively short period of computing time.

The results obtained highlighted a good agreement between the transmission line model and the moment's method.

References

- [1] Aanandan CK, Nair KG. Compact broadband microstrip antenna. *Electron Lett.* 1986, 22:1064–1065.
- [2] Kumar G, Gupta KC. Nonradiating edges and four edges gap-coupled multiple resonator broad-band microstrip antennas. *IEEE Trans Antennas Propag.* 1985, 33:173–178.
- [3] Zhang XX, Song Q. A study on wideband gap-coupled microstrip antenna arrays. *IEEE Trans Antennas Propag.* 1995, 43:313–317.
- [4] Hongming A, Nauwelaers KJC, Van de Capelle AR. Broadband active microstrip antenna design with the simplified real frequency technique. *IEEE Trans Antennas Propag.* 1994, 42:1612–1619.
- [5] Lee RQ, Lee KF. Experimental study of the two-layer electromagnetically coupled rectangular patch antenna. *IEEE Trans Antennas Propag.* 1990, 38:1298–1302.
- [6] Liu Z, Kooi P, Mook-Seng L. A method for designing broad-band microstrip antennas in multilayered planar structures. *IEEE Trans Antennas Propag.* 1999, 47:1416–1420.
- [7] Legay H, Shfal L. New stacked microstrip antenna with large bandwidth and high gain. *IEE Proc.* 1994, H141:199–204.
- [8] Rahim. M. K. A and Gardner. P. The design of Nine Element Quasi Microstrip Log-periodic Antenna. *IEEE RF and Microwave Conference 2004*, 5 -6 October 2004, pp. 132- 135.
- [9] Rahim. M. K. A, Ahmad. M. R, Asrokin. A and Aziz. M. Z. A. A. 'The Design of UWB antenna using log Periodic Technique. *Loughbrough Antennas and Propagation Conference (LAPC 2006)*, 2nd - 3rd April 2006, Loughbrough, U.K.

